UNITED NATIONS EDUCATIONAL, SCIENTIFIC AND CULTURAL ORGANIZATION
INTERNATIONAL ATOMIC ENERGY AGENCY
INTERNATIONAL CENTRE FOR THEORETICAL PHYSICS
I.C.T.P., P.O. BOX 586, 34100 TRIESTE, ITALY, CABLE: CENTRATOM TRIESTE

SMR/930 - 41

"Workshop on El Niño, Southern Oscillation and Monsoon"
15 - 26 July 1996

"Interactions between Regional and Planetary Scale Circulations & Interannual Variability of Indian Summer Monsoons"

H. ANNAMALAI & B.N. GOSWAMI
Centre for Atmopsheric Sciences
IISC
Bangalore, India

Interactions Between Regional and Planetary scale circulations and Interannual Variability of Indian Summer Monsoon

H Annamalai and B N Goswami,

Centre for Atmospheric Sciences,

Indian Institute of Science,

Bangalore 560 012.

INDIA.

e-mail: goswamy@vigyan.iisc.ernet.in

ABSTRACT

The primary objective of the present study is to elucidate the physical mechanism through which the planetary scale circulation associated with El Nino-Southern Oscillation (ENSO), affects the interannual variability (IAV) of the Indian monsoon. The other major objective is to identify the role of regional scale circulations on the IAV of the Indian monsoon. To study the individual and collective roles of the planetary and regional scale circulations in modulating the IAV of the Indian monsoon, we use the monthly zonal and meridional winds at six levels from the ECMWF analysis and SST data for the period 1980-1991. The domain of analysis covers the tropical Indian and Pacific oceans. The analysis is carried out with a hypothesis in mind. As in the intraseasonal oscillations (Goswami, 1994) it is proposed that the IAV of monsoon precipitation over land is governed by a competition and interaction between an oceanic heat source, observed over the equatorial Indian ocean and a continental heat source, observed over the Indian continent during the monsoon season. An initial examination of the ECMWF analysis revealed an unphysical trend that was removed using an objective technique. To decipher the 3-D structure of the combined variability we have used the multivariate empirical orthogonal function (MEOF) analysis. This technique combined with the removal of the unphysical trend in the data has shown that the physical modes associated with the planetary and regional scale circulations are separable and paved the way to bring out clearly the physical mechanism through which ENSO affects the monsoon.

The first three modes (MEOFs 1-3), representing the planetary scale component, together explain 52% of the domain averaged variance and are associated with the ENSO forcing. The spectra of all the three common coefficient time series (PCs) are dominated by a quasi-four year oscillation (LF). The modes (MEOFs 4-6) totally explaining 15.5% of the domain averaged variance are associated with regional scale circulations. All the spectra of PCs(4-6) are dominated by a quasi-biennial oscillation (QBO). The vertical structure of the planetary scale modes is baroclinic but that of the regional scale modes is quasi-barotropic. It has

been demonstrated that the planetary scale modes, associated with ENSO forcing, favour and modulate mainly the oceanic heat source over the equatorial Indian ocean while the regional scale modes favour and modulate the continental heat source. It is shown that the effect of ENSO is largely confined to the oceanic heat source. This is primarily because, during ENSO events, the shift of the Walker circulation results in more net moisture convergence over the equatorial belt, enhancing the oceanic precipitation and suppressing the continental precipitation. Thus ENSO influences monsoon indirectly by favouring the oceanic heat source which in turn influences the continental one through induced subsidence.

Although the regional scale modes explain only 15.5% of the domain averaged variance, it is shown that their contribution is infact larger than the planetary scale modes over the Indian continent and is comparable over the equatorial Indian ocean in many years. Another important result is that the anomalies associated with the regional scale modes peak during boreal summer. These results indicate that the regional modes are responses of the monsoon heat source. Whether the monsoon will be 'good' or 'bad' in a particular year depends crucially on the phases of the LF and QBO modes. This explains why in some year the Indian monsoon may be 'good' (as was the case in 1994) while there may be an El Nino in Pacific.

1. Introduction

In the last few years a number of studies have made serious attempts to simulate the interannual variability (IAV) of Indian summer monsoon (e.g. Palmer et al., 1992, Zwiers, 1993, Sperber et al., 1994, Chen and Yen, 1994, WMO, 1993, 1994) and to hindcast seasonal mean monsoon rainfall (Brankovic et al., 1994, Shukla and Fennessy, 1994) using different atmospheric general circulation models (AGCMs). The status and prospects of the seasonal forecasting has recently been reviewed by Palmer and Anderson (1994). This high level of interest in the prediction of the seasonal monsoon and its interannual variation is partly based on the premise (Charney and Shukla, 1981, Shukla, 1981) that the low frequency tropical variability is mainly forced by slowly varying boundary conditions such as sea surface temperature (SST), snow cover etc. Many AGCM studies forced with observed SST as boundary conditions have established that the IAV in most of the tropics is primarily governed by the observed SST. This result coupled with the fact that some coupled GCMs (CGCMs) are now capable of predicting the SST 6-12 months advance (see Latif et al., 1994 for a review) has further enhanced the optimism for long range dynamical prediction of the seasonal means in the tropics.

In particular regard to the Indian monsoon, two important observations may be made from these studies on simulation of IAV and predictability. Firstly, most models can simulate the IAV of some planetary scale component or circulation associated with the monsoon such as the divergent circulation (as given by the velocity potential) or the monsoon shear index (as defined by Webster and Yang (1992)). However, the simulation of the IAV of the monsoon rainfall differs widely from one model to another (Sperber and Palmer, 1994) indicating the great sensitivity of this part of regional circulation on resolutions and physical parameterizations of the models. The second observation is that while the prediction of seasonal mean rainfall over other parts in the tropics (e.g. Sahel or equatorial Pacific) do not seem to be sensitive to small changes in the initial conditions, the simulation of seasonal mean Indian monsoon rainfall seems to be quite sensitive to small changes in the initial conditions (Palmer and Anderson, 1994). This may indicate that the seasonal mean monsoon circulation in the tropics may be unique and that it is not entirely forced by slowly varying boundary conditions (SST) but is also partly governed by internal dynamics. Some other models, on the other hand, do not observe such sensitivity of the simulation of the seasonal mean monsoon on initial conditions (Shukla and Fennessy, 1994). Thus, the sensitivity of the seasonal mean monsoon rainfall may be related to individual AGCM's monsoon precipitation climatology. Unfortunately, most AGCMs currently do not simulate the monsoon precipitation climatology realistically. Therefore, further careful experimentation will be required to establish clearly the dependence of the simulation of seasonal mean monsoon on initial conditions.

The main interannual signal in the SST (boundary condition for the atmosphere) is the Pacific SST variations associated with the El Nino and Southern Oscillation (ENSO). That there is a relation between ENSO related SST changes in the Pacific and Indian monsoon rainfall has been known since early twenties (Walker, 1924). However, the contemporaneous relationship between Pacific SST and Indian summer monsoon has been rather weak (Rasmusson and Carpenter, 1983, Shukla and Paolino, 1983, Yasunari, 1990). An examination of the simultaneous relationship between Pacific SST and Indian Summer monsoon over the last century reveals that (Mooley and Shukla, 1987) while a large number of droughts in India tend to occur with ENSO in Pacific, there are several droughts that occurred without an ENSO in Pacific. Moreover there are many years where there were above normal rainfall (eg. 1994, 110% of normal rainfall in India) while there was an ENSO evolving in Pacific. These observations lead us to believe that while the ENSO SST has a modulating effect on the monsoon rainfall, it is not the dominating one. It appears that there are competing factors (may be due to internal dynamics and of regional character) that may have comparable influence.

Why the ENSO SST does not have a dominating influence on the monsoon rainfall is likely to be related to the physical mechanism through which ENSO SST influence Indian monsoon rainfall. Unfortunately, this is still a controversial subject. Although several studies (eg. Webster and Yang, 1992, Nigam, 1994) have attempted to clarify the physical connection

between the two, it is far from clear at this point. While most variations of precipitation in the equatorial region is related to an east-west movement of the precipitating zones (ITCZ) which is associated with the east-west movement of the Walker circulation, the Indian summer monsoon is associated with a gigantic north south movement of the ITCZ. The special shape of the continent and the position of the Himalayas produce a favourable location for the ITCZ over the land during northern summer. However, the waters to the south-south east are still warm ($\geq 28°C$) with a maximum close to the equator and hence also favours an oceanic ITCZ (Goswami et al., 1984). As an outcome, it is a competition between the two ITCZs that determine the precipitation over the continent. This competition results in the intraseasonal oscillations (ISO) of the monsoon and manifest in the northward propagation of the ITCZ (Sikka and Gadgil, 1980, Gadgil, 1988, Goswami, 1994). As a result of this competition during the whole monsoon season (June-September), the ITCZ resides over the continent for a longer period than over the ocean resulting in the precipitation maximum over the land. However, the signature of the oceanic ITCZ can be seen even in the climatological June-July-August (JJA) mean precipitation with some precipitation still over the equatorial Indian Ocean. Because of this special feature the Indian monsoon is unique as compared to the other tropical circulations. Therefore, the interaction between ENSO and monsoon must necessarily take this special feature of monsoon into account. In the language of dynamical systems, the two favorable positions of the ITCZ may be considered as two 'attractors' of the system (Palmer, 1994). The system tends to reside in one attractor for some time before a perturbation pushes it out to the other attractor where it tends to reside for some time leading to the intraseasonal oscillations. This process is governed by internal dynamics and may have limited predictability. The IAV of the seasonal mean monsoon is governed not by detailed evolution of the individual ISO but by the statistics of them (eg. frequency of occurrence, mean amplitude etc). The statistics of the ISO may be modulated by the large scale environment created by the slowly varying boundary conditions such as that associated with ENSO. It is believed that it is through such a modulation of the ISO, the ENSO influences the IAV of the monsoon. Some recent modelling studies (Fennessy and Shukla, 1994) support this perspective where it is shown that the spatial patterns of both the intraseasonal and interannual of simulated monsoon are similar. The objective of the present study is to bring out clearly the physical mechanism through which ENSO influences the monsoon. This is done by examining the three dimensional pattern of the large scale response associated with ENSO related SST. We do this by conducting a multivariate empirical orthogonal function (MEOF) analysis employing the singular value decomposition (SVD) technique. The interaction between the ENSO and monsoon is then interpreted keeping in mind the climatological picture described above.

As mentioned earlier and as will be shown by our analysis, the modulation of the monsoon circulation by the ENSO related forcing is rather weak. This brings in the possibility of some regional oscillations contributing significantly to the interannual variations of the monsoon rainfall. Such a regional scale oscillation may arise due to some regional scale forcing or due to some internal dynamical processes. There are some positive SST anomalies during JJA in the equatorial Indian Ocean associated with ENSO variations. That is a part of the ENSO forcing. Once that part is taken out, the remaining SST anomalies in the Indian ocean are rather weak and are unlikely to constitute a strong regional forcing. Apart from SST, other feedback processes such as soil moisture and radiation similar to one proposed by Meehl (1990, 1994) may also give rise to some internal oscillations of the monsoon with a period of about 2 years. In addition, there is a possibility that modulation of the intraseasonal oscillations such as the 30-50 day mode by the annual cycle can also give rise to a quasi-biennial oscillation (Goswami, 1995). The fact that these intraseasonal oscillations have largest amplitude in the Indian ocean and western Pacific sector lends support to this possibility. In a recent study of a multi year run of an AGCM with climatological annual cycle of SST repeating every year as boundary condition it has been shown that the monsoon system can oscillate with a period of about two years without any external forcing at this period (Goswami and Manabe, 1995, manuscript under preparation). This oscillation has a regional character with anomalies that are consistent with an oscillation of the monsoon heat source. The second objective of the present study

is to bring out the observed structure and characteristics of such regional scale circulations associated with the monsoon without going into details of their physical origin. This is again done through the MEOF analysis. It is shown that such a MEOF analysis allows us to separate out the large scale oscillations from the smaller regional scale oscillations. Once, the large scale and regional scale oscillations are separated, we study their individual and collective contributions to the interannual variability of the monsoon.

The paper is organized as follows. In section 2, we describe the data used and the methodology employed in this study. In this section we also show that the European Center for Medium Range Forecasting (ECMWF) analysis for the period 1980-1991 has a significant unphysical trend arising out of changes in the model and the analysis system. We propose an objective method of removal of this trend and show that the detrended data is still useful for interannual variability studies. The three dimensional (3-D) structure of the large scale response associated with ENSO is brought out through a MEOF analysis in section 3. Based on the structure of this response, the physical mechanism through which ENSO influences the monsoon precipitation is elucidated. In section 4, we examine the 3-D structure of the regional scale modes and compare them with the structure of the large scale oscillations (associated with ENSO). In this section we also indicate how these regional scale oscillations may be related to the fluctuations of the monsoon heat source. The differences in the vertical structures of the regional and planetary scale modes are also brought out. In section 5, we show how the regional and the planetary scale modes contribute to the interannual variability of the monsoon. Section 6 contains a summary of the results with some concluding remarks.

2. Data and Method used

2.1. Data processing

The primary data used in the present study are the monthly means of operationally analysed winds from the ECMWF, for the period 1980-1991. To extract the horizontal and vertical structures associated with the planetary and regional scale circulations, we use both the zonal and meridional winds at six standard pressure levels namely, 1000 mb (surface), 850 mb, 700 mb, 500 mb, 300 mb and 200 mb. The horizontal resolution of this data is 2.5° × 2.5°. In addition we use SST and air temperature data for the same period. This data comes from COADS for the period 1980-1987 and from the CAC blended SST data for 1988-1991. This data set is in a 2° × 2° horizontal resolution. We have also made use of the Florida State University (FSU) surface stress analysis (Goldenberg and O'Brien, 1981) as an independent analysis to compare ECMWF surface wind analysis. This data set is also in a 2° × 2° horizontal resolution. For convenience of our analysis, we have interpolated all the data into a 5° longitude ×4° latitude horizontal resolution. Since we are interested in the IAV patterns, all the variables are subjected to a 5 month running mean filter.

It has been recognized that the model based operational analysis, like NMC and ECMWF, have some serious deficiencies when used for interannual variability studies (Trenberth and Olson, 1988). The three major reasons for these deficiencies are, (a) gradual improvement of the models' both resolution and physical parameterizations, (b) frequent changes in data assimilation system and (c) unavailability of delayed mode data. The ECMWF model has grown from a 15 level 1.875 grid point version in 1980 to a 19 level spectral model with triangular 213 resolution in recent times. The most significant change in the analysis system is the introduction of multivariate optimum interpolation and diabatic nonlinear normal mode initialization in mid eighties. Trenberth and Olson (1988) note that the major model change to the ECMWF analyses on May 1, 1985, significantly increased the divergent part of the tropical wind. So it is expected that due to both the model and analysis changes, the archived data include unphysical jumps at different points of time history. Thus it becomes imperative that we try to isolate these unphysical variation in the ECMWF analysis before conducting any diagnostic studies on IAV and predictability. Trenberth and Guillemot (1994) have concluded that the ECMWF analysis should be used with due care for any IAV studies. Many recent studies like Wang (1992), Murakami and Matsumoto (1994) have utilized the ECMWF data sets without paying attention to the inherent problems in the data. A more detailed study on the

fundamental issue, objective ways to overcome it, and the usefulness of the corrected analysis in IAV studies is reported in Goswami and Annamalai (1995). A brief summary is presented here.

Since our main interest is to bring out the interaction between the planetary scale Walker circulation and regional scale monsoon circulations, we examine the time series of anomalies of zonal wind shear ($U_{850}-U_{200}$) averaged over the NINO4 ($5°S-5°N, 160°E-150°W$) (Fig 1a), and the meridional wind anomalies averaged over the equatorial Indian ocean ($5°S-5°N, 60°E-90°E$) (Fig 1b). It may be noted that the climatology of each field at each grid point for each calendar month was constructed by averaging over all the 12 years. Anomalies are then calculated subtracting the climatology corresponding to the given month from the actual observation for the particular month.

A clear trend is seen in both the time series of Fig 1 (a,b). The anomalies prior to mid eighties tend to be of one sign while those in the later period tend to be of the opposite sign. This is basically due to the shift in the climatologies which is attributable to the major changes in the model and analysis system in the mid eighties. It is felt that if this unphysical trend is not removed from the data, there is a real danger of misinterpretation of the results. We present here an unique and objective way of removing the trend in the ECMWF fields.

To examine how the trend is manifested in the large scale part of the circulation, we carried out a multivariate EOF analysis (described in detail later in this section). In Fig 1 (c,d,e) we show the dominant PCs which have significant trend. Also shown is the slope obtained from least squares fit. The anomalies tend to change sign somewhere in mid eighties. Our suspicion is that this trend is related to the change in the analysis system (including model changes and analysis-initialization changes). However, in order to establish whether this trend is unphysical or not we must compare this data to an independent analysis that does not depend on the model based analysis system. No such data set for upper air variables is available. As we discuss later in this section that MEOF analysis brings out the interrelated variability patterns. If we have independent analysis of one variable, comparison between patterns of variability of this variable with those of the corresponding variable in the multivariate analysis will help us identify the systematic error that are common to all variables. We do it by comparing with the FSU analysis of the surface winds over the tropical Pacific. The dominant PCs of FSU data set do not show trend (not shown). Moreover, when we compared the spatial patterns (EOFs) of the FSU with that of the 1000 mb ECMWF winds, we noted some spurious unphysical patterns in the ECMWF analysis. Thus it is clear to us that the trend in the ECMWF analysis is unphysical. We now discuss briefly the objective means of removing this trend

We detrended the PC 1, PC 2 and PC 5 (see fig 1) by fitting a straight line using least squares methods. The fields are then reconstructed using the detrended PCs. Then we conducted a MEOF analysis and found that there was neither any spurious spatial patterns nor any trends in the dominant PCs (sections 3 and 4). Good agreement between patterns in the detrended surface wind and those of the independent FSU data set indicate that, even though the climatology may have been wrong during the period prior to 1985, the large scale part of the interannual anomalies during that period may still be reasonable. The time evolution of the dominant PCs of the detrended analysis also agrees well with that of the PCs of the FSU winds. This indicates that major interannual variations are captured in the detrended analysis. It is also seen that the objectively detrended anomalies as discussed above are nearly identical to anomalies constructed with respect to two climatologies, one for the period 1980-1985 and another for the period 1986-1991. This established that the trend was indeed due to shift in the climatology from prior to 1985 to post 1985 period. Further details of this method of data processing can be seen in Goswami and Annamalai (1995). For our main analysis described below, we use only the detrended wind fields. We also carried out a MEOF analysis with the anomalies constructed with respect to the two climatologies. We found that both the spatial and temporal patterns are 'identical' to those obtained from the detrended wind fields.

2.2. Multivariate EOF analysis

To decipher the recurrent patterns of combined variability in both horizontal and vertical

structures, we conduct a MEOF analysis employing the SVD technique (Nigam and Shen, 1993, Wang, 1992). As we mentioned before, we use SST and zonal and meridional winds at all the six levels. All the variables are normalized using their individual spatial variance (Nigam and Shen, 1993) before the analysis. This method provides a more efficient way of compacting a large volume of multifield data, as in our case. As geophysical fields are not only correlated spatially but also correlated amongst each other, this technique brings out the coherent patterns that are highly inter-related. This unique feature helps us to bring out the 3-D recurrent patterns of anomalies associated with certain types variability leading insight into the dynamics of such variability. From the inspection of the spatial patterns and the PCs one can separate out the modes corresponding to large scale and small scale variabilities, which is of prime importance in the context of the present study

As mentioned, the singular values obtained from the MEOF analysis of all the variables is shown in Fig. 2. An inspection of this figure shows that the first six singular values are above the noise floor (North et al., 1982) and the eigenmodes corresponding to them are physical and realistic. Since our analysis involves a large volume of multifield data, the stability of both the temporal and the spatial patterns are validated by the following approach. First we carried out a MEOF analysis with SST and the zonal and meridional winds at 1000 mb, 850 mb and 200 mb only. Next the zonal and the meridional winds at all the six levels and the SST are combined in the MEOF analysis. The eigenvalues and the temporal patterns and the spatial patterns of 1000 mb, 850 mb and 200 mb winds are found to be identical in both the cases. Thus, we feel that the MEOF patterns described here are robust and stable.

3. Horizontal and Vertical structures of the Planetary scale modes

In this section we discuss the combined spatial and temporal structures of the planetary scale oscillations associated with ENSO related SST forcing. We shall show that these patterns are such that they result in a modulation of the oceanic heat source over the equatorial Indian ocean which in turn affect the interannual variations of the Indian monsoon.

The first three dominant modes, totally explaining about 52% of the domain averaged interannual variance, are identified as responses of ENSO related planetary scale modes. The identification is based on the spatial patterns, the common coefficient time series (PCs) and their corresponding spectra. It is apparent from Fig. 3 that all the first three PCs show pronounced warming/cooling during major ENSO events (eg. 1982/1983, 1987/1988) and their corresponding spectra mainly represent a low frequency (LF) oscillation with the characteristic period of ENSO, i.e., around 4 years. We discuss in some details the horizontal and vertical structures of these three modes (Figs 4-6) and their net effect on the Indian monsoon circulation. The combined spatial patterns of all the seven variables (SST, vector winds at 1000, 850, 700, 500, 300 and 200 mb levels) alongwith the vorticity at 850 mb level are shown. As the MEOFs are calculated using the zonal and meridional components of the wind as two different variables (section 2), their individual EOF patterns are used to construct the vector wind patterns of each MEOFs.

The MEOF1 SST pattern, covering the entire equatorial central and east Pacific (80°W – 160°E) with a maximum around 130° W and symmetric about the equator, captures the basinwide warming associated with the ENSO. As expected, the western Pacific exhibits a slight cooling. It is rather interesting to note that the entire tropical Indian ocean shows warming pattern albeit much weaker (1/6 compared to that of east Pacific). Associated with this SST pattern, strong westerly anomalies can be found over the central and east Pacific at surface, 850 mb and 700 mb levels. The stronger winds are observed at 700 mb at low level. Concurrently, easterly anomalies, weakening the climatological monsoon westerlies at lower levels, prevail over the equatorial Indian ocean. The wind patterns in the lower three levels show the presence of a prominent 'divergence' cell around the maritime continent which is associated with the cooler SST during a warm phase of the ENSO. Two cyclonic circulations symmetric about the equator and centred around 15°, one in the northern hemisphere (NH) and the other in the southern hemisphere (SH) are also apparent at 850 mb over the Pacific ocean. This is clearly seen in the relative vorticity at 850 mb which shows two strong vortices, engulfing the entire Pacific ocean. The two cyclonic vortices at lower levels on either side of the equator are consistent with response of the atmosphere associated with enhanced precipitation in the central and eastern Pacific during a warm phase of the ENSO. It is rather interesting to note that somewhat weak vortices of the opposite sense to that observed over Pacific are seen over the equatorial Indian ocean indicating the wavenumber one type large scale response associated with this mode.

In the vertical, the phase transition of the wind patterns begins at 500 mb. The strong equatorial westerly anomalies over the Pacific are replaced by weak easterly anomalies. However, the sub-tropical winds in both the hemispheres have strengthened at this level. Over the Pacific, two gigantic anticyclones centered around 15° in both hemispheres are particularly prominent in the next vertical level, (300 mb). These structures attain their maximum strength at 200 mb level. At these levels the entire tropical Indian ocean is replaced by strong westerly anomalies again weakening the climatological easterly jet in this region. Also prominent is the 'convergence' zone around the maritime continent overlaying the 'divergence' zone around the same longitudes at 850 mb. Arkin (1982) in his analysis of 200 mb winds for the period March 1969 to February 1979 also found similar patterns in the dominant EOF mode. After estimating the cross-correlation between the EOF wind patterns and Pacific SST, he concluded that the patterns are ENSO related. As the MEOF analysis used here brings out only the interrelated patterns, an examination of the SST pattern associated with the dominant mode clearly shows that this coupled pattern is ENSO related. The horizontal and vertical structure of MEOF1 patterns are basically the response of the atmosphere due to a strong equatorial heat source over the central equatorial Pacific during the warm phase of the ENSO (Gill, 1980). By bringing out the inter-related patterns among the oceanic and atmospheric variables, we are able to document the strong air-sea coupling over the tropical Pacific. It is clear from Fig. 4 that the atmospheric response due to ENSO in the dominant mode is baroclinic in vertical structure.

The SST pattern of MEOF2 (Fig. 5) represents warming over the central and western

Pacific and cooling over the eastern Pacific and south Indian ocean. The warming is well spread meridionally (about 18° in both hemispheres) unlike in MEOF1 SST. Associated with this SST patterns, strong westerly anomalies are seen in the west-central Pacific at low levels. The common coefficient time series PC2 leads PC1 by about 8 months. Keeping in mind the patterns of MEOF1 and MEOF2, the eastward migration of the coupled anomalies during the evolution of the strong warm episodes (eg. 1982-1983) can be clearly seen. We further note that such an eastward migration of anomalies are not present during 1987-1988.

The wind anomalies over the Indian ocean are in phase with that over the East Pacific but out of phase with that over the west Pacific at all pressure levels. One interesting observation is that there is an appreciable amount of wind flow over the Indian ocean and reaching a maximum over the equatorial Indian ocean. However, they do not penetrate into the Indian continent. This pattern is best seen in 700 mb. The vorticity field at 850 mb shows two cyclonic circulations, one in the NH and the other in the equatorial SH, over the Indian and eastern Pacific regions. These patterns are out of phase with those found in the western Pacific. This is again consistent with the heating distribution associated with the SST distribution. This pattern too has a wavenumber one zonal structure with somewhat shorter meridional scale compared to the MEOF1.

In the vertical, again we see the phase transition taking place at 500 mb level. The cyclonic and anti-cyclonic patterns seen at the low levels are accompanied by their respective counterparts at higher levels with higher intensity. One major feature at both 300 mb and 200 mb is the penetration of the Pacific trade winds into the monsoonal region; resulting in a very strong interaction between these two regions. As mentioned earlier, both in MEOF1 and MEOF2, we find that over the Indian ocean regions, maximum wind anomalies are over the equatorial sector.

The third mode, MEOF3 (Fig. 6), also representing a LF oscillation, further shows that over the Indian ocean the wind anomalies at the low levels have a strong cross-equatorial flow and have their maximum strength at the equator. There is an appreciable veering of the wind into

the Indian continent. This cyclonic vorticity over the northern Indian ocean is accompanied by an anti-cyclonic vorticity over the north western-central Pacific. At low levels, over the Pacific, two anticyclones symmetric about the equator are apparent. One intriguing fact is that the spatial pattern associated with MEOF3 is out of phase with that of MEOF1. This indicates that some fraction of the variance in the LF oscillation tend to oppose the dominant pattern of the ENSO related forcing in the tropical sectors. Another interesting point to note is that while the structure of the two vortices over the Indian ocean reverse their sign above 500 mb the two vortices in the Pacific associated with MEOF3 retains the same sign upto 200 mb. Thus at higher levels they tend to strengthen MEOF1 pattern. The low level vorticity has maximum amplitude over the Indian ocean domain. The wind patterns at higher levels show strong easterlies over the monsoon region and again having maximum strength at the equatorial zone. One can also see the penetration of the Pacific trade winds into the monsoon domain. So in effect, all the three modes representing the LF oscillation in the tropical sector, show a strong interaction between the Pacific trade winds and the monsoon winds. We discuss now the salient features of these results and the physical mechanism through which ENSO affects the monsoon.

It is well recognized that monsoon is a direct circulation forced by deep tropospheric heat sources (Goswami, 1994). Though radiation plays a role in selecting the location of the heat sources, these heat sources are basically maintained by organized deep convection driven by moisture convergence. As mentioned in the Introduction, the monsoon precipitation over the land is governed by the competition between an oceanic and a continental heat source. We find from the results presented so far that all the three ENSO related modes favours a net enhancement of cyclonic vorticity over the equatorial Indian ocean. Also we find that the ENSO effect on the vorticity over the land is weak. As a result, the effect of ENSO will be manifested as more boundary layer moisture convergence over the oceanic heat source rather than over the continental one. This results in enhancement of precipitation over the Indian ocean region. Within the conceptual framework of monsoon variability discussed in the introduction, this tend to suppress continental convection resulting in reduced continent precipitation. Many AGCMs, when forced by observed SST, simulate more mean precipitation over the oceanic region (Palmer et al., 1992, WMO, 1994). Also it is seen that the monsoon shear index defined by Webster and Yang (1992) is highly correlated with ENSO but is unrelated to the precipitation over India. This is because this shear index arises as a response of the atmosphere to the oceanic heat source or ITCZ. Many recent studies (eg. Ju and Slingo, 1994) use the shear index as a measure of Asian monsoon in assessing the performance of an AGCM. As termed by Webster and Yang (1992), this is indeed a measure of the large scale (planetary scale) component of the monsoon that may be related to ENSO. However, it does not represent any part of the regional scale monsoon. Therefore, this index by itself is only a part of the story and should not, in our opinion, be used as the sole index of IAV of the Indian monsoon. Having identified that the manifestations of ENSO related heating affects the oceanic heat source, we now discuss the circulation patterns that affect the continental heat source.

4. Horizontal and vertical structure of the regional scale modes

In this section we present and discuss the combined spatial and temporal patterns of the regional scale oscillations associated with forcings other than related to ENSO. We shall show that these structures favor and dominate the IAV of the continental heat source, which is equally if not more important for the monsoon precipitation over land.

The modes MEOF4, MEOF5 and MEOF6 totally explain about 15.5% of the domain averaged interannual variance. As before, they are identified as non-ENSO forcings based on the spatial patterns, the PCs and their corresponding spectra. It is apparent from Fig. 7 that the spectra of all the PCs mainly contain an oscillation in the biennial range. We recall that the spectra of the MEOF1, MEOF2 and MEOF3 mainly contain a quasi-four year oscillation. Thus, this method of analysis has automatically separated the structures associated with these two frequencies known to be present in tropical low frequency variability (Rasmusson et al., 1990,

Barnett, 1991). The spatial patterns of these modes show smaller scale regional structures unlike the basinwide influence seen in Figs 4-6. This is best seen in the vorticity at 850 mb, showing more small scale meridional as well as zonal structures.

The SST pattern of MEOF4 (Fig. 8) has appreciable amplitude over the central Pacific and north eastern Indian ocean. Apart from this, there are also some small scale fluctuations in other parts of the domain of analysis. The vorticity field at 850 mb shows a cyclonic vortex pair around the equator over the Indian region, together with an anticyclonic vortex pair around the equator in the central Pacific sector. In addition there is another cyclonic vortex in the north west India. Such a scenario is best seen in the northern summer months (Krishnamurti, 1970) over the tropical domain. One important observation is that the strength of the continental vortex over India is stronger than that of the vortex seen in the equatorial Indian ocean. As a result of existence of these two vortices, the cross equatorial flow tends to be rather weak. What is more intriguing and interesting is the quasi-barotropic nature of the vertical patterns associated with this mode upto even 300 mb level. Sikka (1977) and Douglas (1992) found that the observed structure of typical monsoon depressions is barotropic upto 250 mb in the vertical. This is further supported by the barotropic nature of the 10-20 day westward moving intraseasonal oscillations during the monsoon season over India (Chen and Chen, 1993). With these arguments, we come to the conclusion that the MEOF4 mode mainly represents the regional scale circulations. Similar features are found in MEOF5 and MEOF6 too.

In MEOF5 (Fig. 9), the SST pattern shows comparable amplitude in both Indian and Pacific domains. The region west of the dateline shows an out of phase structure with that to the east of the dateline. The temperature pattern over the Indian continent has large amplitudes. Associated with these heating patterns, the winds at the low levels have cyclonic circulation in the north Indian ocean as depicted by the vorticity field at 850 mb. This pattern over Indian region is associated with an anticyclonic vorticity over the north mid-Pacific. Similar patterns are obtained for MEOF4 also. The cyclonic vortex over the Indian region is strongest at 500 mb level. In the vertical plane, this mode is barotropic even upto 200 mb, with a tilt in the position of the circulation pattern with height towards north-northeast. Such a barotropic structure is consistent with the vertical structure of typical monsoon depressions and lows, which collectively make up the monsoon heat source.

The other small scale mode MEOF6 (Fig. 10) brings out the traditional monsoonal flow at low levels in the Indian ocean basin. The uniqueness of this mode is that the winds show a pronounced maximum away from the equator over the north Indian ocean region. The vorticity picture at 850 mb clearly shows strong cyclonic vorticity over the Indian continent and off the Somali coast, while the equatorial Indian ocean shows an opposite vorticity structure. Though there are appreciable vortices in the Pacific domain, the strength is maximum over the monsoon domain. As seen in the previous regional scale modes, this mode too is barotropic till 300 mb in the vertical. Consistent with the other regional modes, there is considerable tilt of the circulations with height. This again agrees with the observed structure of the mean vorticity fields during northern summer (Krishnamurti, 1970).

Thus, all the three regional scale modes, representing a QBO in the tropical sector, indicate that they may be associated with fluctuations of the monsoonal heat source. In association with the QBO of the monsoon, there appears to be simultaneous oscillations in some parts of the Pacific. While the monsoon heat source is influenced by land surface processes and orography, the origin of the heat sources in the Pacific is mainly related to the SST fluctuations in this time scale over that regions. Since the regional scale modes are responsible for the vortices off the Somali coast and over the Indian continent, we may conclude that they are associated with the continental heat source. It has been recently shown that to have realistic simulation of the mean monsoon precipitation in an AGCM, the monsoon trough should be simulated realistically (Fennessy et al., 1994). In other words, the continental vortex should be simulated realistically. While, we feel that the LF quasi four year variability of the monsoon (the oceanic heat source) is due to the LF variability of the tropical SST, the quasi-biennial variability of the monsoon (the land heat source) may be due to some internal dynamics. The continental heat source with a QBO is likely to be related to the observed QBO in the observed

all India monsoon rainfall. In a recent study of the all India monsoon rainfall series for the period 1901-1980, Annamalai (1995) found that the biennial component explains about 31%, whereas the LF frequency component accounts for 10% of the total variance. So the IAV of the monsoon depends crucially on the interactions between the LF oscillations of the oceanic heat source and the QBO of the continental heat source.

5. Interaction between Planetary and Regional scale modes in modulating the IAV of monsoon

As mentioned in Sections 3 and 4, the IAV of monsoon must result from

(a) the fluctuations of the oceanic heat source associated with the LF frequency IAV (b) the fluctuations of the continental heat source associated with the QBO variability (c) and their interactions. Also it has been noted earlier that the fluctuations of these heat sources are basically caused by the fluctuations of the moisture convergence above the boundary layer and the ability of that moisture to reach the lifting condensation level. So before directly dwelling into the question of interactions, we briefly recap the factors that influence the fluctuations of the moisture convergence over these two heat sources. More details of this can be seen in Goswami (1994).

The moisture convergence for the oceanic heat source is governed by

(a) moisture convergence due to large scale convergent circulation in the near equatorial region or due to boundary layer frictional convergence associated with a large scale cyclonic vorticity (b) cloud-radiation feedback (c) evaporation from regional SST anomalies and (d) interaction between dynamics and organized convection (Goswami and Shukla, 1984). The large scale convergence in the equatorial region is governed by (1) subsidence from the continental heat source, this way the continental and oceanic heat sources interact, (2) by the global 30-50 day eastward propagating oscillation and (3) convergence associated with a shift of the Walker circulation (section 3).

The moisture convergence for the continental heat source is governed by (a) large scale convergence in the monsoon trough region and also subsidence from the oceanic heat source (b) cloud-radiation feedback (c) evaporation associated with land surface processes and (d) convergence produced by midlatitude waves. In the case of the oceanic as well as continental heat sources, the large scale convergence is also associated with a cyclonic vorticity. The large scale cyclonic vorticity makes it possible for the low level converged moisture to reach the level of lifting condensation and allows it to form a deep heat source. We find that the fluctuations and interactions between these two heat sources are governed by several complex interactions. It is not feasible from observations to separate out the contributions from the individual physical processes. However, the net effect of these physical processes which result in the low level vorticity structures will give us a definite picture on the interactions between the two heat sources.

We present in Fig 11, the composite vorticity at 850 mb for good minus bad monsoons over the longitude domain $40°E-140°E$. The good monsoons considered are 1983 and 1988, while the bad monsoons are 1982 and 1987. It should be noted here that only the four monsoon months (July through September) are used to construct the composites. In the four panels shown, the first one corresponds to the observed total vorticity anomalies at 850 mb. As expected, strong cyclonic vorticity prevails over the Indian continent oriented along the monsoon trough. The turning of the westerly jet results in a cyclonic vorticity over the Somali jet area. Anticyclonic vorticity basically dominates the southern equatorial Indian ocean. The weak cyclonic vorticity in the equatorial Indian ocean over the warm waters starting from about 70° E eastward is a signature of the oceanic heat source. During good monsoon, it is weaker than the continental one. In the next panel, we show the total effect of the planetary scale vorticity anomalies obtained by $MEOF1 \times PC1 + MEOF2 \times PC2 + MEOF3 \times PC3$. It is quite apparent that the vorticity structures dominate the equatorial Indian ocean sectors. It has less strength over the continent. However, the total effect of the regional scale vorticity anomalies obtained by $MEOF4 \times PC4 + MEOF5 \times PC5 + MEOF6 \times PC6$, shows the dominance of the vorticity field over the Indian continent and off the Somali coast. The fourth panel shows the

sum of large scale plus regional scale vorticity. There are two main features in this figure. Firstly, it is very close to the total anomaly shown in the first panel. This shows that the first six modes are nearly sufficient to describe the observed IAV. Secondly, the continental vortex seen in the total anomaly is almost entirely due to the regional components only (third panel) and only very modest vorticity anomaly is contributed by the large scale components over the Indian continent. On the other hand, the planetary as well as the regional scale circulation make comparable contributions to the equatorial heat source.

Before going into the details of the interactions between the heat sources, we present the composites of the vertical structure of the wind patterns. This is shown in Figs 12a-e. The traditional monsoonal flow, strong cross-equatorial flow, the Somali jet and the flow over the continent is best seen in the total observed anomalies at 850 mb level. It is noteworthy that large amount of cross-equatorial flow is seen at both the low levels essentially in the regional scale composites with winds exhibiting cyclonic turning around Bay of Bengal. This is consistent with a response to a continental heat source. The planetary scale, composites at 850 mb also show a weak cross-equatorial flow but strong winds at the equator and convergence towards the equator. This scenario is consistent with the fact that the an equatorial heat source is largely responsible in driving the winds associated with these modes. The sum of large scale and regional scale anomalies shown in the last panel is very close to the total observed pattern. We also note that the large scale LF circulation dominates the composites at almost all levels over the Pacific with the regional scale QBO mode playing a secondary role. This is consistent with the findings of Rasmusson et al., (1990). As seen in the MEOFs structures, along the vertical the large scale anomalies tend to change their phase at about 500 mb. However, the regional scale cyclonic circulations can be seen upto 300 mb. The real physical mechanism for this vertical structure of the regional heat source is not clear to us at present. But this must be related to the structure of the vertical heating profile. More work is needed to substantiate these findings.

It is important to note at this point that although the regional scale EOFs explain only

15.5% of the total area averaged variance, their contribution over the Indian continent is, in fact, larger than the three planetary scale modes which together explain 52% of the area averaged variance. Over the equatorial Indian ocean too, the contribution of the regional scale modes is comparable to that of the planetary scale modes. This statement is further substantiated below. To examine the interactions and competition in more details, we show in Fig 13a, the time-latitude section of the vorticity field at 850 mb averaged between the longitudes $70^\circ E - 90^\circ E$. Throughout the period of analysis, the large scale vorticity shows an apparent northward propagation of anomalies and one can also observe that the major dipole centres are located around $10^\circ S$ and $10^\circ N$ in almost all the years. This picture clearly shows that the large scale circulation has a very weak response over the Indian continent. It can also be noted that the anomalies have their maximum strength in the beginning of the calendar months. On the other hand, the time-latitude section of the regional scale modes (Fig 13b) shows dominating vortices over the land areas. Also the contribution of this regional scale modes are comparable in magnitude to that of the large scale modes over the oceanic belts in some years. One very interesting feature is that in almost all the years, the anomalies peak during the boreal summer months. This further strengthens our arguments that the MEOFs 4-6 may be responses of monsoon related heat sources. To bring out more clearly the collective role of the large and regional scale processes in determining the total vorticity we construct the vorticity field of large+regional scale modes and present it in Fig 13c. It is evident that during the bad monsoons of 1982 and 1987, cyclonic vorticity is dominating the oceanic belts, whereas anticyclonic vorticity is seen over the continent. In the good monsoons of 1983 and 1988 the opposite picture is evident. Let us now examine the interactions in some details.

In 1982 boreal summer, both the large scale and regional scales show cyclonic (anticyclonic) vortices over the equatorial Indian ocean (over the Indian continent). This indicates that the oceanic heat source which is favored by the large scale forcing is further enhanced by the regional scale forcing or in other words both the oscillations are in phase. During 1983 summer, the large scale part tends to change into anticyclonic vorticity over the oceanic belt

low rather than monsoon convective heating over the continent and Bay of Bengal. Quite interestingly the planetary modes (panel b) captures more convection over the oceanic region and the regional scale modes (panel c) indicate more convection over the continental region with decrease of convection over the equatorial Indian ocean again consistent with our picture. The continental negative OLR anomaly, however, does not appear to be related to the deep convection associated with the monsoon heat source. The deep convection and the monsoon heat source is found around $(20^\circ N, 90^\circ E)$ during monsoon season. Such problems in OLR data representing the surface heating over the continental regions has also been noticed earlier (Chelliah and Arkin, 1992). Due to these inherent problems we have not used the OLR data in our MEOF analysis. We found that inclusion of the OLR data in the MEOF analysis introduces some spurious (unphysical) patterns in the wind.

6. Summary and Conclusions

The main objective of the present study is to elucidate the physical mechanism through which ENSO (planetary scale circulation) affects the interannual variability of the monsoon. Our another objective is to identify and assess the role of the regional scale circulations in modulating the interannual variability of the monsoon and to study their interactions with their planetary scale counterpart. These objectives are achieved by an analysis of the 3-D observations and isolating the combined variability using a multivariate EOF analysis.

The primary data used in the present study are the monthly means of operationally analysed winds from the ECMWF, for the period 1980-1991. We have used the zonal and meridional winds at 1000 mb, 850 mb, 700 mb, 500 mb, 300 mb and 200 mb. In addition, we have also used the SST (COADS and CAC) for the same period. The domain of analysis covers the tropical Indian and Pacific oceans. It has been demonstrated that the ECMWF analysis has an unphysical trend arising out of changes in both model and analysis system. An objective way has been proposed to remove this trend and the detrended data has been found to be realiable for interannual variability studies. To decipher the recurrent 3-D structure of combined variability, we have used the multivariate EOF analysis. This unique technique has brought out some interesting results which have provided new insight into the dynamics of interannual variability of the monsoon. The first six recurrent combined spatial and temporal structures obtained from the MEOF analysis represent physical modes. The interesting aspect of these results is the separation of the physical modes corresponding to the quasi-four year oscillation (LF) and the physical modes corresponding to the quasi-biennial oscillation (QBO). It may be recalled that these two oscillations dominate the tropical low frequency variability (Rasmusson et al., 1990).

Based on the examination of their large scale spatial structures, their common coefficient time series (PCs) and their corresponding spectra, the first three modes (MEOFs 1-3) are identified as those associated with ENSO forcing. These three modes together explain about 52% of the domain averaged variance. The spectra of all three PCs are dominated by a quasi-four year period. The vertical structure of these planetary scale modes is baroclinic and the phase transition takes place at around 500 mb level. The other three modes (MEOFs 4-6), totally explaining about 15% of the domain averaged variance are related to regional scale circulations. This is supported by the spatial structures and the spectra of the corresponding PCs. The spectra of all these three PCs (PCs 4-6) are dominated by a quasi-biennial oscillation. However, the vertical structure of these regional scale modes is quite different from that of the planetary scale modes. It is found to be quasi-barotropic even upto 300 mb. The physical reasons for this scenario is not clear to us at present but it is felt that this must be related to the vertical heating profile. These may also partly be due to the fact that these circulation features are associated with off-equatorial heat sources often associated with land processes.

The conceptual picture of the monsoon variability is related to the strength and competition of the two heat sources, one over the equatorial Indian ocean and the other over the Indian continent. From the composites of good minus bad monsoons, we found that the planetary scale modes with a LF quasi-four year variability associated with the ENSO forcing, favour and modulate the oceanic heat source (ITCZ). Quite interestingly, the regional scale modes

having a QBO variability (which may be a result of internal dynamics), favour and modulate the continental heat source. It is also found that this heat source is responsible for the winds off the Somali coast, Bay of Bengal and into the continent. These two observations lead us to hypothesize that the net moisture convergence over the oceanic heat source is significantly modulated by the planetary scale circulations while the net moisture convergence over the Indian continent is mainly due to the regional scale circulations. Thus it is clear to us that the effect of ENSO on monsoon is basically confined to the oceanic ITCZ. We conclude that this the basic reason for the no-correlation of the monsoon shear index of Webster and Yang (1992) with the Indian monsoon rainfall. The ENSO influences the interannual variability of the monsoon indirectly through interaction between the two ITCZs.

It is not feasible from observations to assess and quantify the various physical processes that are responsible for the moisture convergence into the two heat sources. Nevertheless, the total effect of these processes can be seen in the vorticity fields at 850 mb. Analysis of the relative vorticity fields at 850 mb showed that there are two cyclonic vortices over the monsoon domain, one associated with the oceanic ITCZ and the other associated with the continental ITCZ. It is seen that during major ENSO events (eg. 1982) both the LF and QBO are in phase over both the oceanic and the continental ITCZ, thus enhancing the oceanic precipitation and suppressing the continental precipitation. In the period of analysis, it is observed that the contribution of the LF variability dominates the oceanic ITCZ during major ENSO events but its effect over the continent is weak. In some years, the contribution of the LF and QBO modes are comparable in magnitude over the oceanic region, but the QBO modes always dominate the vorticity field over the Indian continent. We also see that the circulations over the ocean and continent associated with the ENSO forcings, have opposite structures throughout the vertical plane. This is further supported by the regional scale modes. These results confirm that the circulation over the equatorial Indian ocean, during monsoon season, tends to oppose the circulation over the Indian continent. We, however, recall that the planetary scale part of the circulation modulating mainly the oceanic heat source oscillates with a quasi-four year period while the regional part modulating the continental heat source oscillates with a QBO. Thus, in a particular year, whether the monsoon will be 'good' or 'bad' depends crucially on the phases of these two oscillations. This explains why in some year while there may be an El Nino in Pacific, the Indian monsoon may be 'good' as was the case in 1994.

The conceptual picture stressed in the introduction is clearly brought out in the present study from observational data sets. We are in a position to conclude that in order to explain the relationship between monsoon and ENSO, the contribution and competition between the planetary scale circulation (ENSO forcing) and the regional scale circulation (may be due to internal dynamics) should be taken into account. We feel that the SST related boundary forcing, for an AGCM, may be able to capture the oceanic ITCZ and hence favor oceanic precipitation more as seen in many AGCMs (WMO, 1994). In order to have a better mean monsoon precipitation simulation, we stress the point that the continental vortex or the monsoon trough, should be simulated realistically.

Acknowledgements

The authors would like to thank V.Krishnamurthy for helping us copy the ECMWF analysis. We thank Department of Science and Technology, Government of India for partial support for this work.

REFERENCES

Annamalai, H. 1995: Intrinsic problems in the seasonal prediction of the Indian summer monsoon rainfall. *Met. Atmos. Phys.*, **55**, 61-76.

Arkin, P. 1982: The relationship between interannual variability in the 200 mb tropical wind field and the southern oscillation. *Mon. Wea. Rev.*, **110**, 1393-1404.

Barnett, T.P., 1991: The interaction of multiple time scales in the tropical climate system. *J. Climate*, **4**, 269-284.

Brankovic, C., T.N. Palmer and L. Ferranti, 1993: Predictability of seasonal atmospheric variations. *J. Climate*, **7**, 217-237.

Charney, J.G and J. Shukla, 1981: Predictability of monsoons. Chapter in 'Monsoon Dynamics', J. Lighthill and R.P. Pearce (Eds), Cambridge University press. pp 99-110.

Chelliah, M and P. Arkin, 1992: Large-scale interannual variability of monthly outgoing longwave radiation anomalies over the global tropics. *J.Climate*, **5**, 371-389.

Chen, T.C and J.A. Chen, 1993: The 10-20 day mode of the 1979 Indian monsoon: Its relationship with the time variation of monsoon rainfall. *Mon. Wea. Rev.*, **121**, 2465-2482.

Chen, T.C and Yen, 1994: Interannual variation of the Indian monsoon simulated by the NCAR community climate model: Effect of the tropical Pacific SST. *J. CLimate*, **7**, 1403-1415.

Douglas, M.W., 1992: Structure and dynamics of two monsoon depressions. Part I: Observed structures. *Mon. Wea. Rev.*, **120**, 1524-1547.

Gadgil, S., 1988: Recent advances in monsoon research with particular reference to the Indian monsoon. *Aust. Met. Mag.*, **36**, 193-204.

Gill, A.E., 1980: Some simple solutions for heat-induced tropical circulation. *Quart. J. Roy. Meteor. Soc.*, **106**, 447-462.

Goldenberg, S.O and J.J. O'Brien, 1981: Time and space variability of tropical Pacific wind stress. *Mon. Wea. Rev.*, **109**, 1190-1207.

Goswami, B.N., J.Shukla, E.K. Schneider and Y.Sud, 1984: Study of the dynamics of

the intertropical convergence zone with a symmetric version of the GLAS Climate model. *J. Atmos. Sci.*, **41**, 5-19.

Goswami, B.N., 1994: Dynamical predictability of monsoons - Problems and prospects. *Proc. Indian. Natn. Sci. Acad.*, **60A**, 101-120.

Goswami, B.N., 1995: A multiple interaction model for the origin of the tropospheric QBO. *J. Climate*, **8**, 524-534.

Goswami, B.N and H. Annamalai., 1995: Origin of an unphysical trend in ECMWF analysis and its objective removal: Importance in interannual variability studies. *Tech. Report, Centre for Atmospheric Sciences, Indian Institute of Science, Bangalore*, 95 AS 2.

Goswami, B.N and J. Shukla, 1984: Quasi-periodic oscillations in a symmetric general circulation model. *J. Atmos. Sci.*, **41**, 20-37.

Fennessy, M.J., J.L. Kinter, B. Kirtman, L. Marx, S. Nigam, E.Schneider, J. Shukla, A Vernekar, Y. Xue and J. Zhou, 1994: The simulated Indian monsoon: A GCM sensitivity study. *J. Climate*, **7**, 33-43.

Fennessy, M.J and Shukla, 1994: GCM simulations of active and break monsoon periods. *Proc. of the international conference on Monsoon variability and prediction. Trieste.* pp 576-585. Vol. 2, WCRP-84, WMO/TD-No 619.

Ju, J and J. Slingo, 1994: The Asian summer monsoon and ENSO. *Submitted to Quart. J. Roy. Meteor. Soc.*.

Krishnamurti, T.N., 1970: Observational study of tropical upper tropospheric motion field during northern hemisphere summer. *Report No. 70-4*. Department of Meteorology, Florida State University.

Latif, M., T.P. Barnett, M.A. Cane, M.Flugel, N.E. Graham, H.von Storch, J.S. Xu and S.E. Zebiak, 1994: A review of ENSO prediction models. *Climate Dynamics.*, **9**, 167-179.

Meehl, G.A., 1990: Seasonal cycle forcing of El Nino-Southern Oscillation in a global coupled ocean-atmosphere GCM. *J. Climate*, **3**, 72-96.

Meehl, G.A., 1994: Coupled land-ocean-atmosphere processes and south Asian monsoon variability. *Science*, **265**, 263-267.

Mooley, D.A., and J. Shukla, 1987: Variability and forecasting of the summer monsoon rainfall over India. *In Monsoon meteorology. (Eds) C.P. Chang and T.N. Krishnamurti*. Monographs on Geology and Geophysics, No. 7.

Murakami, T and J. Matsumoto, 1994: Summer monsoon over the Asian continent and western north Pacific. *J. Meteor. Soc. Japan*, **72**, 719-745.

Nigam, S., 1994: On the dynamical basis for the Asian summer monsoon rainfall- ENSO relationship. *J. Climate*, **7**, 1750-1771.

Nigam, S and H.S. Shen, 1993: Structure of oceanic and atmospheric low-frequency variability over the tropical Pacific and Indian oceans. Part I: COADS observations. *J. Climate*, **6**, 657-676.

North, G.R, T.L. Bell, R.F. Cahalan and F.J. Moeng, 1982: Sampling errors in the estimation of empirical orthogonal functions. *Mon. Wea. Rev.*, **110**, 699-706.

Palmer, T.N, C. Brankovic, P. Viterbo and M.J. Miller, 1992: Modeling interannual variations of summer monsoons. *J. Climate*, **5**, 399-417.

Palmer, T.N and D. Anderson, 1994: The prospects for seasonal forecasting - A review paper. *Quart. J. Roy. Meteor. Soc.*, **120**, 755-793.

Rasmusson, E.M., X. Wang and C.F. Ropelewski, 1990: The biennial component of ENSO variability. *J. Mar. Sys.*, **1**, 71-96.

Rasmusson, E.M and T.H. Carpenter, 1983: The relationship between eastern equatorial Pacific sea surface temperature and rainfall over India and Sri Lanka. *Mon. Wea. Rev.*, **111**, 517-528.

Shukla, J, 1981: Dynamical predictability of monthly means. *J. Atmos. Sci.*, **38**, 2547-2572.

Shukla, J and D.A. Paolino, 1983: The southern oscillation and long range forecasting of the summer monsoon rainfall over India. *Mon. Wea. Rev.*, **111**, 1830-1837.

Shukla, J and M.J. Fennessy, 1994: Simulation and predictability of monsoons. *Proc. of the international conference on Monsoon variability and prediction, Trieste*. pp 567-575. Vol. 2, WCRP-84, WMO/TD-No 619.

Sperber, K.R and T.N. Palmer, 1994: Atmospheric model intercomparision project: Monsoon simulations. *Proc. of the international conference on Monsoon variability and prediction, Trieste* pp 601-608. Vol. 2, WCRP-84, WMO/TD-No 619.

Sikka, D.R, 1977: Some aspects of the life history, structure and movement of monsoon depressions. *Pure. Appl. Geo. Phys.*, **115**, 1501-1529.

Sikka, D.R and S. Gadgil, 1980: On the maximum cloud zone and the ITCZ over Indian longitudes during the southwest monsoon. *Mon. Wea. Rev.*, **108**, 1840-1853.

Sperber, K.R, S. Hameed, G.L. Potter and J.S. Boyle, 1994: Simulation of the northern summer monsoon in the ECMWF model. Sensitivity to horizontal resolution. *Mon. Wea. Rev.*, **122**, 2461-2481.

Trenberth, K.E and J.G. Olson, 1988: An evaluation and intercomparison of global analyses from the National Meteorological Centre and the European Centre for medium range forecasts. *Bull. Amer. Meteor. Soc.*, **69**, 1047-1058.

Trenberth, K.E and C.J. Guillemot, 1994: The total mass of the atmosphere. *J. Geo. Phys. Res.*, **99**, 23, 079-23, 088.

Walker, G.T., 1924: Correlation in seasonal variations of weather III: The local distribution of monsoon rainfall. *Mem. Indian. Met. Dept.*, **23**, 23-40.

WMO, 1993: Simulation and prediction of monsoons - Recent results (TOGA/WGNE, Monsoon Numerical experimentation group, New Delhi, India, 12-14 January, 1993). WMO/TD-No 546.

WMO, 1994: Proc. of the International conference on monsoon variability and prediction. (International centre for Theoretical Physics, Trieste, Italy, 9-13 May, 1994) WMO/TD-No 619.

Yasunari, T., 1990: Impact of Indian monsoon on the coupled atmosphere/ocean system in the tropical Pacific. *Met. Atmos. Phys.*, **44**, 29-41.

Zwiers, F.W., 1993: Simulation of the Asian summer monsoon with the CCC GCM-1. *J.*

Climate, 6, 470-486.

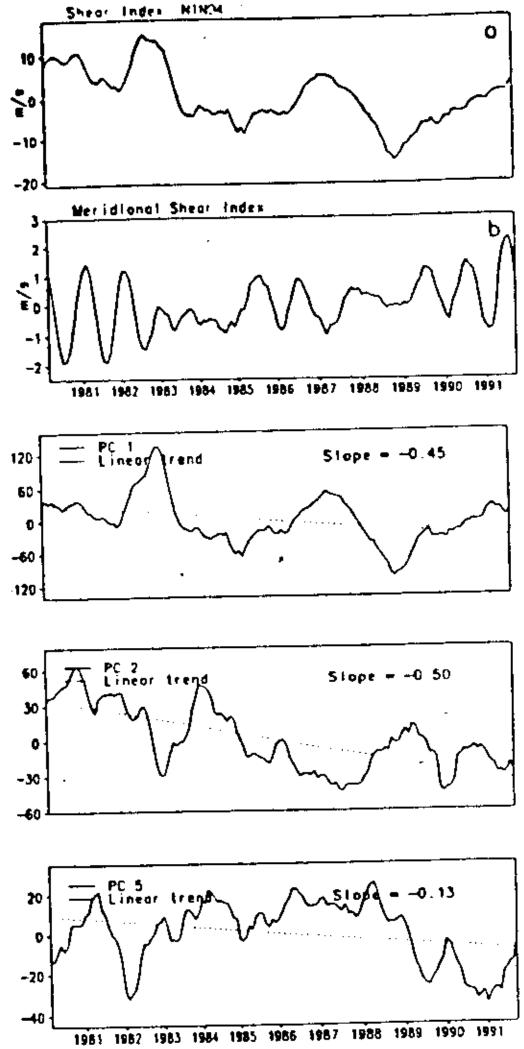

Figure 1: Anomaly time series, based on the 1980-1991 climatology.

(a) the shear index, $(U_{850} - U_{200})$ averaged over the NINO4 $(5°S - 5°N, 160°E - 150°W)$ region in the Pacific.

(b) the meridional shear index, $(V_{850} - V_{200})$ averaged oevr the equatorial Indian ocean $(10°S - 10°N, 40°E - 110°E)$.

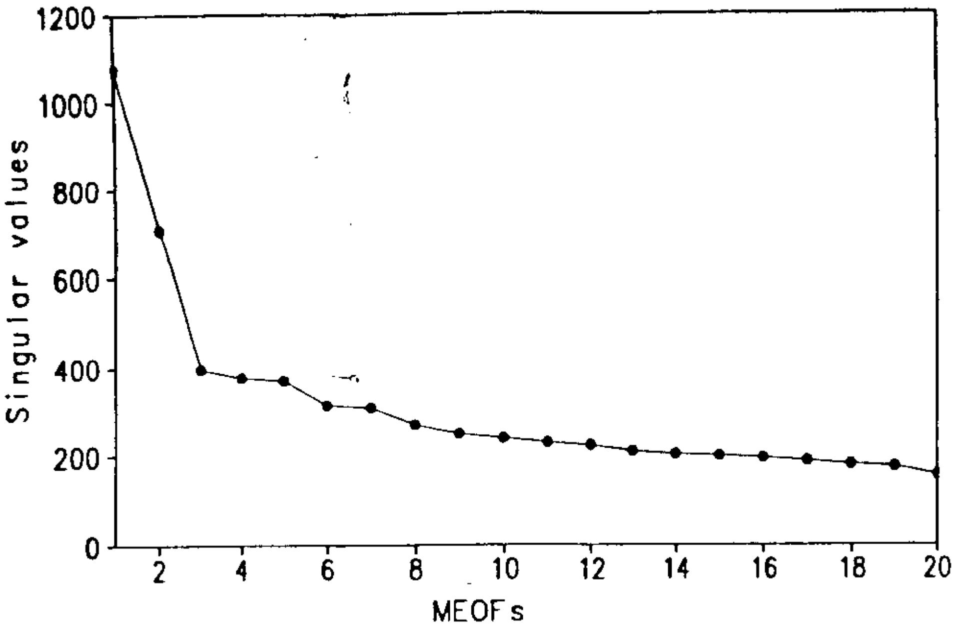

Figure 2: The first twenty singular values of the MEOFs obtained from singular value decomposition technique.

GrADS: COLA/UMCP

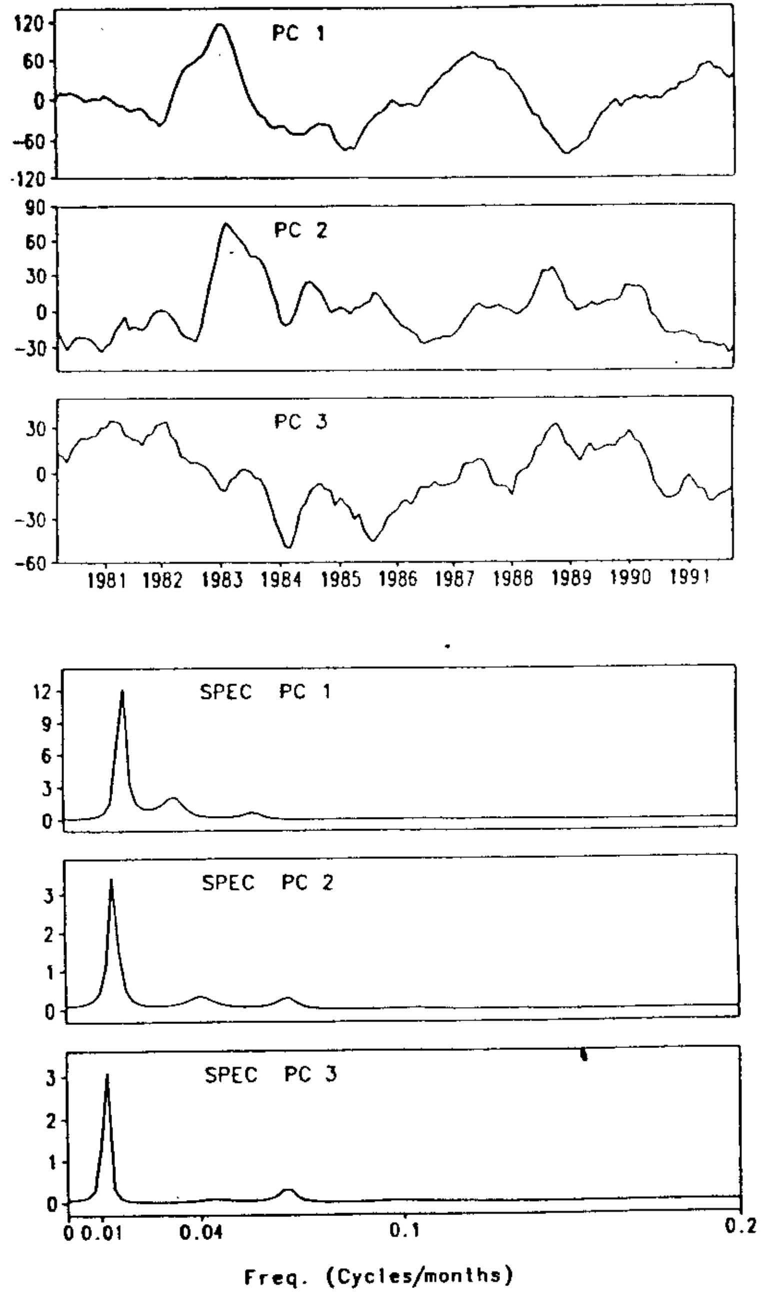

Figure 3: The first three dominant common coefficient time series (PCs) and their corre-

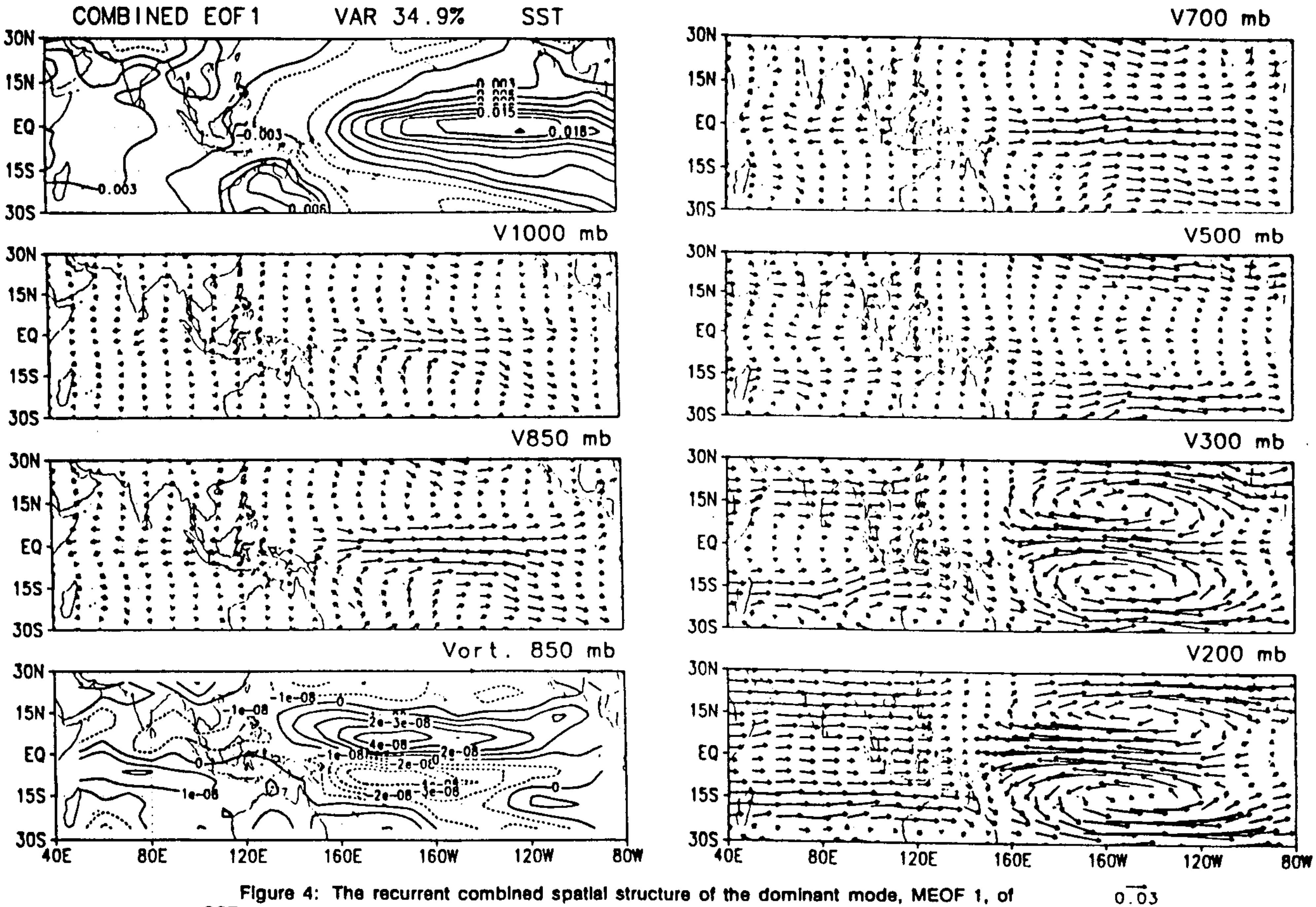

Figure 4: The recurrent combined spatial structure of the dominant mode, MEOF 1, of SST and winds at 1000 mb, 850 mb, 700 mb, 500 mb, 300 mb and 200 mb levels. The MEOFs are calculated using the zonal and meridional components of the wind as two different variables and their individual EOF patterns are used to construct the vector wind patterns. For

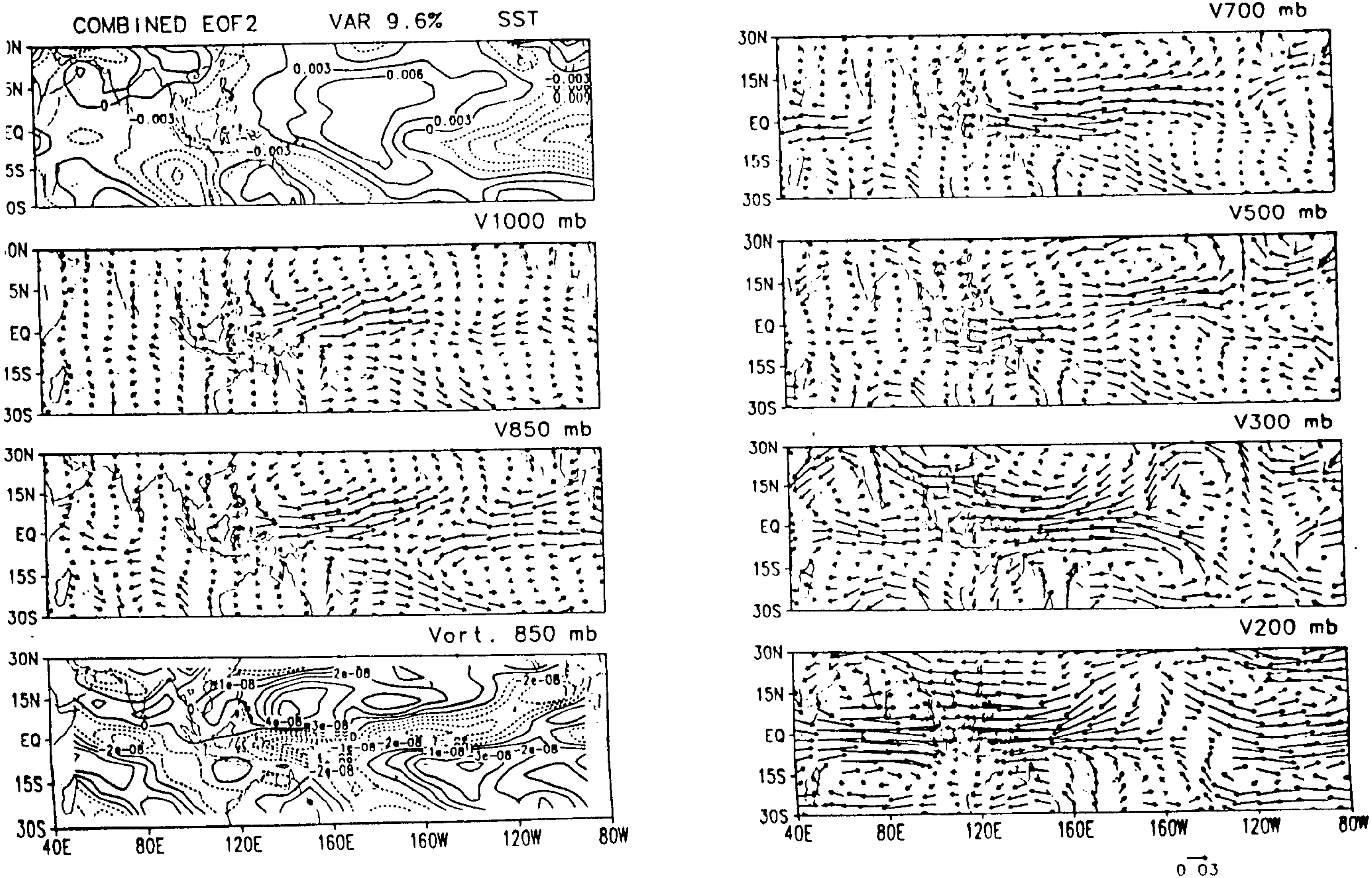
COMBINED EOF2
VAR 9.6%
SST
0.003
0.006
-0.003
0
V1000 mb
V850 mb
Vort. 850 mb
2e-08
-2e-08
1e-08
4e-08
3e-08
-1e-08
-3e-08
V700 mb
V500 mb
V300 mb
V200 mb
30N
15N
EQ
15S
30S
40E
80E
120E
160E
160W
120W
80W
0.03

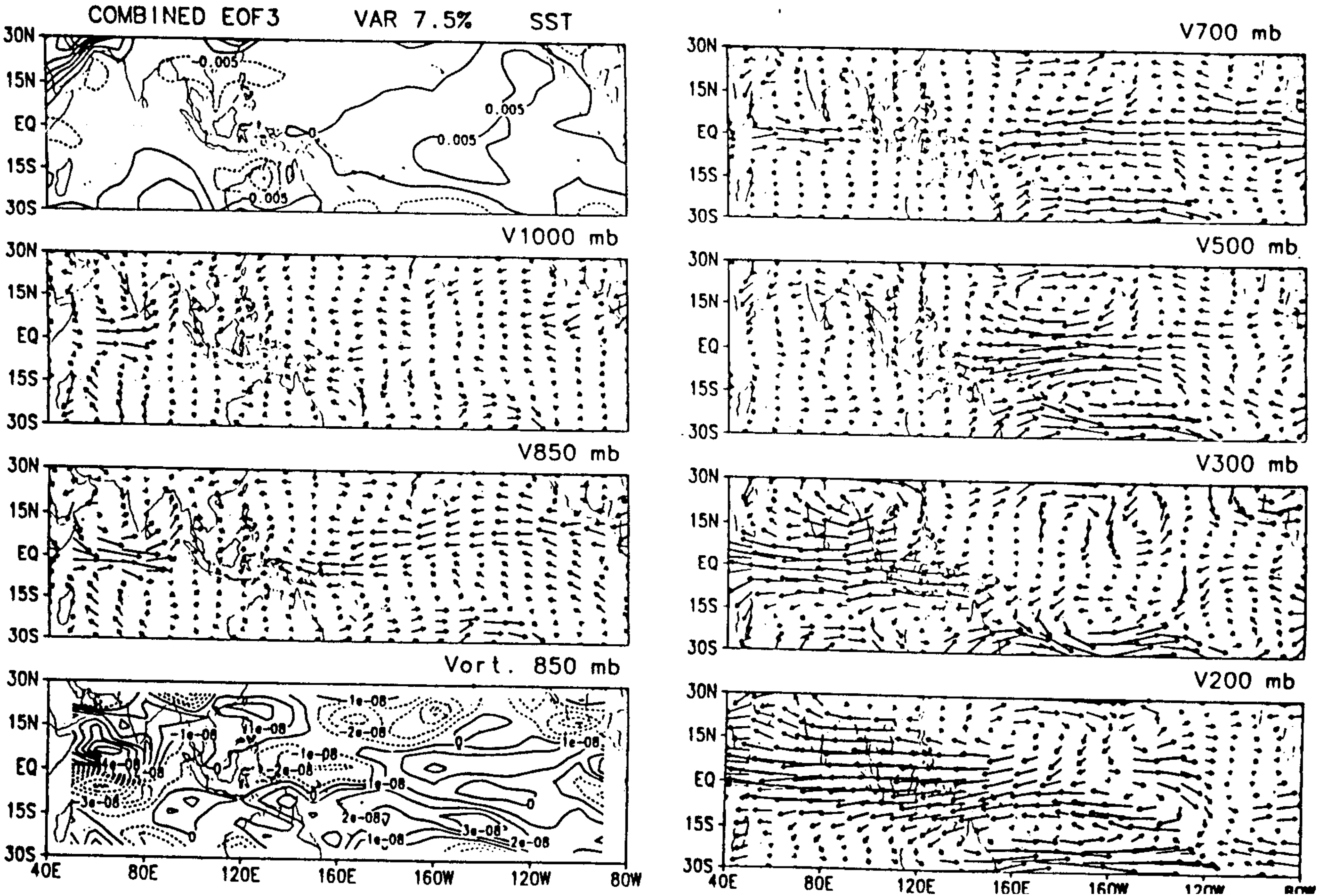

COMBINED EOF3
VAR 7.5%
SST
V1000 mb
V850 mb
Vort. 850 mb
V700 mb
V500 mb
V300 mb
V200 mb
30N
15N
EQ
15S
30S
40E
80E
120E
160E
160W
120W
80W
-0.005
0.005
0
1e-08
-1e-08
-2e-08
2e-08
3e-08

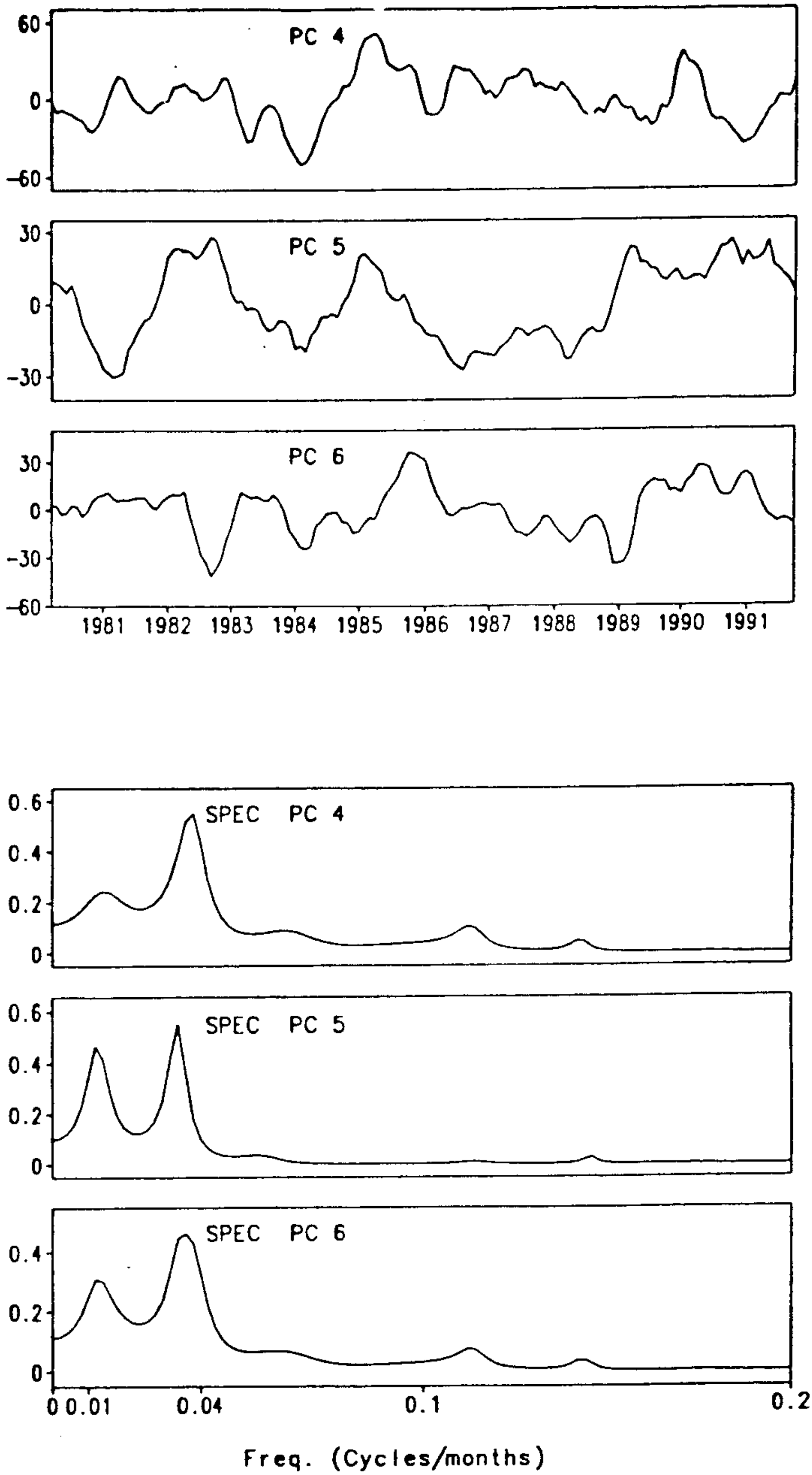

Figure 7: Same as Figure 3 but for PCs (4-6).

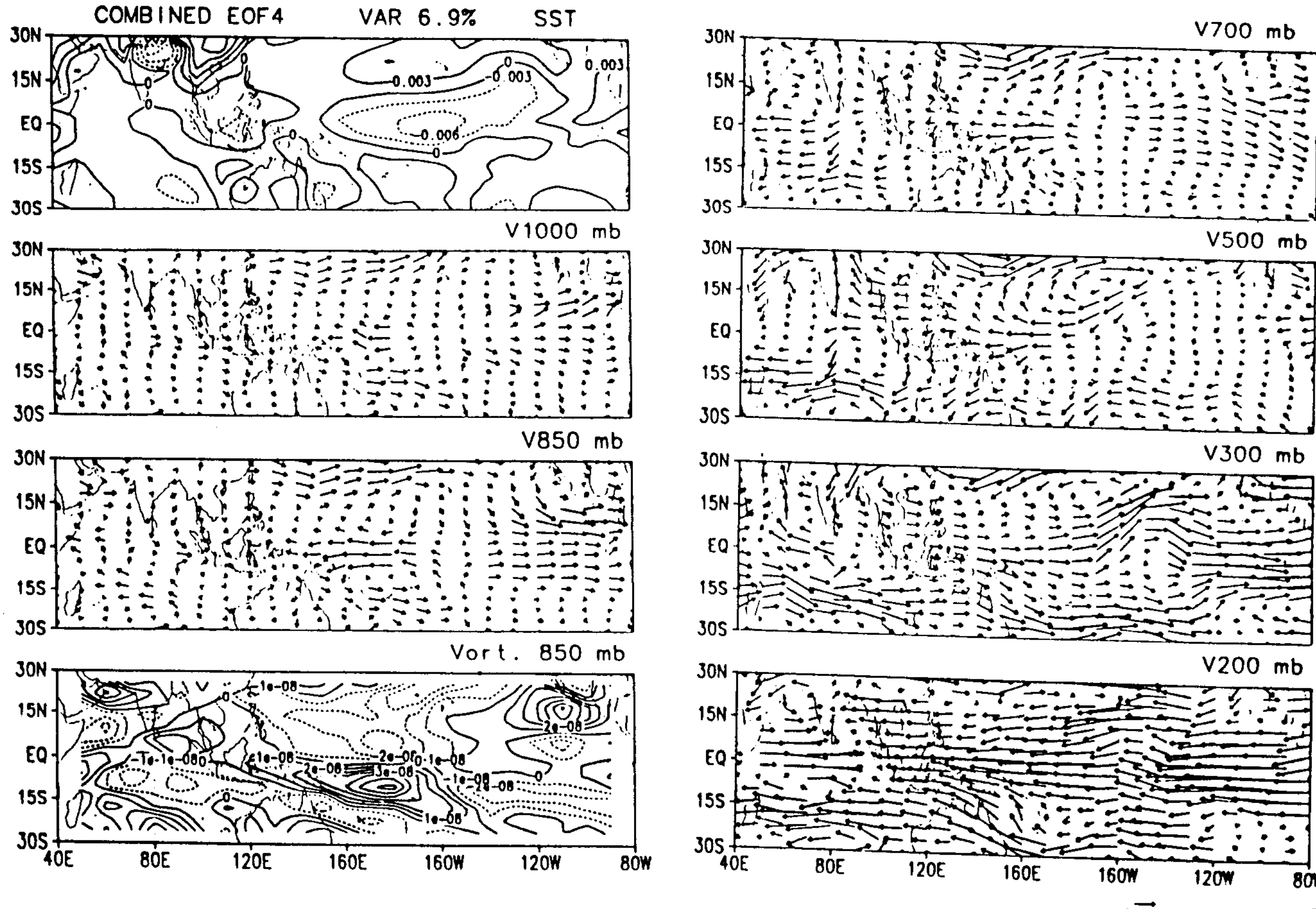

Figure 8: Same as Figure 4 but for MEOF 4.

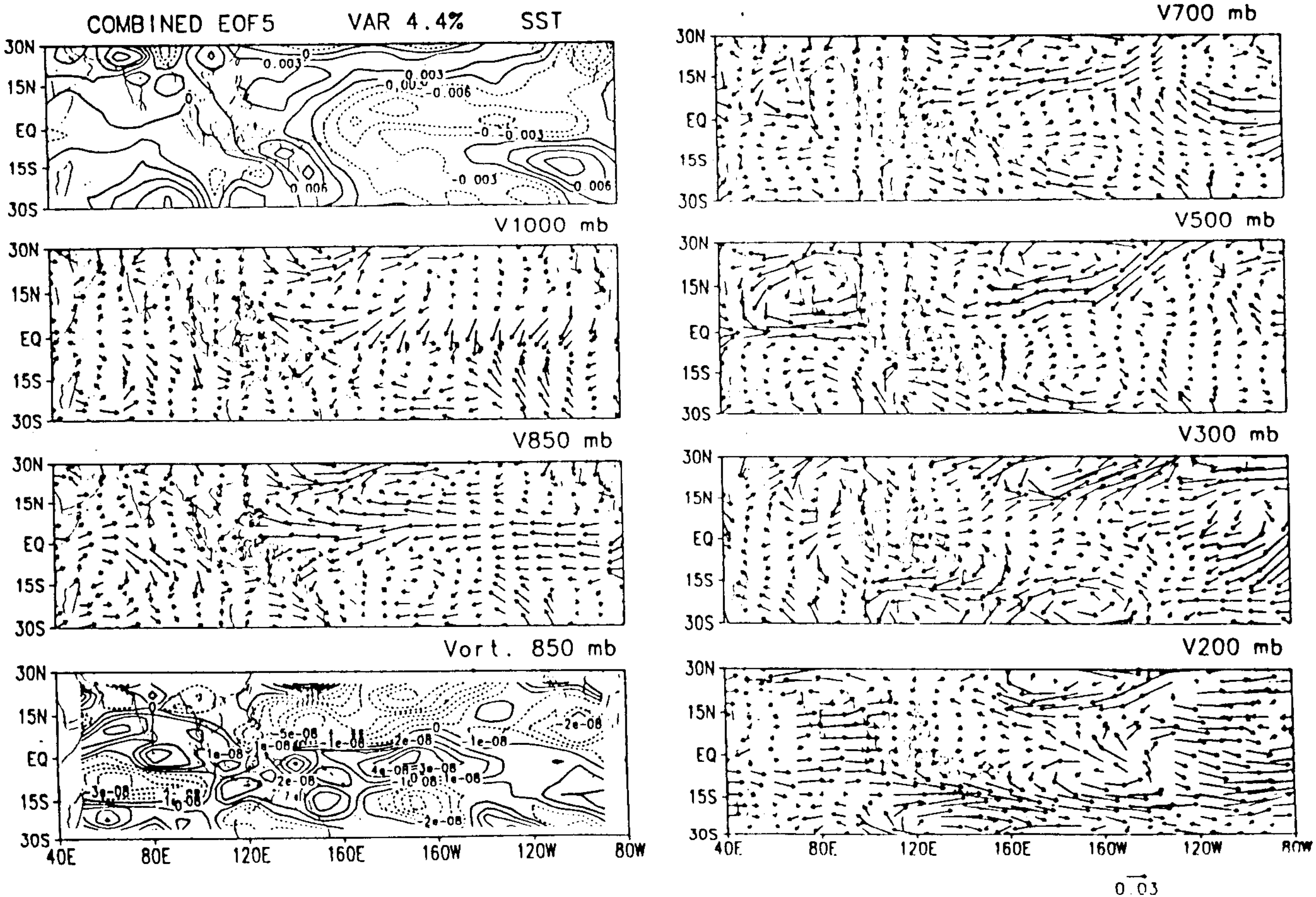

COMBINED EOF5
VAR 4.4%
SST
V1000 mb
V850 mb
Vort. 850 mb
V700 mb
V500 mb
V300 mb
V200 mb
30N
15N
EQ
15S
30S
40E
80E
120E
160E
160W
120W
80W
0.03

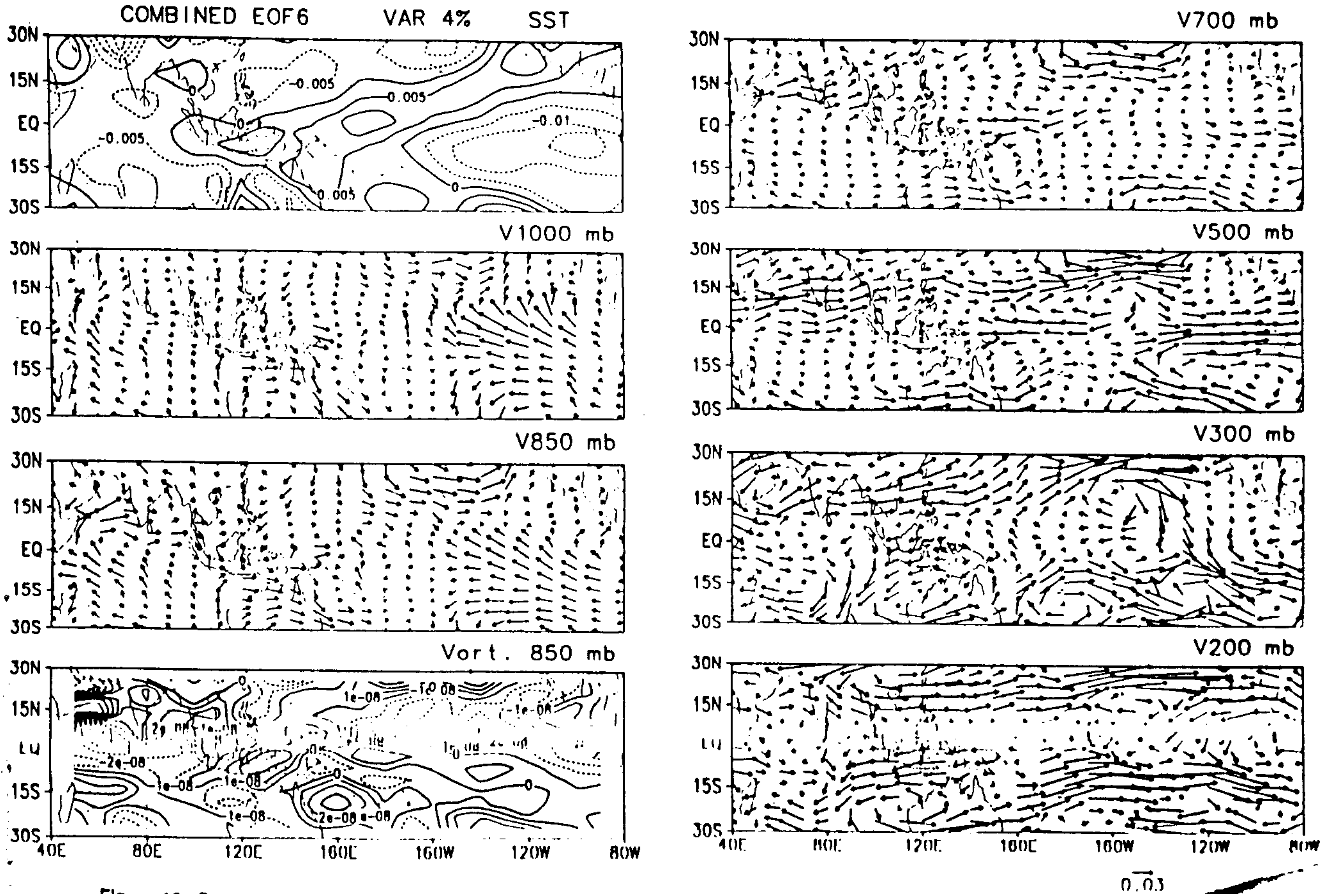
COMBINED EOF6
VAR 4%
SST
V700 mb
V1000 mb
V500 mb
V850 mb
V300 mb
Vort. 850 mb
V200 mb
30N
15N
EQ
15S
30S
-0.005
0.005
-0.01
0
1e-08
-2e-08
40E
80E
120E
160E
160W
120W
80W
0.03

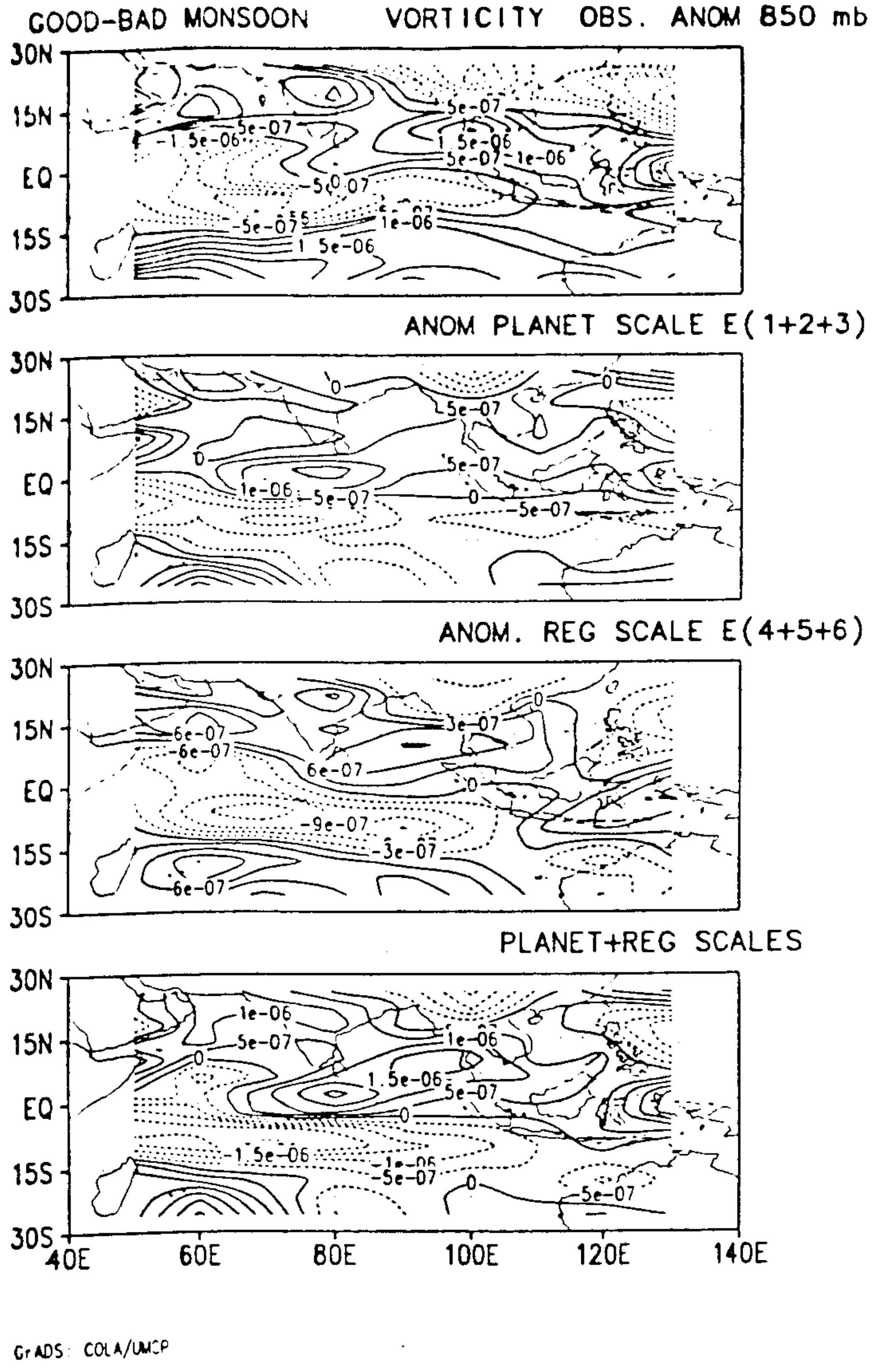

Figure 11: Composites of good minus bad monsoons for the relative vorticity at 850 mb.

Good monsoons considered are 1983 and 1988, while the bad monsoons are 1982 and 1987. Note that only the four monsoon months (JJAS) are used to construct the composites.

Panel (a): observed vorticity anomaly (b): contribution due to planetary scale modes $[MEOF1 \times PC1 + MEOF2 \times PC2 + MEOF3 \times PC3]$ (c): contribution due to regional scale

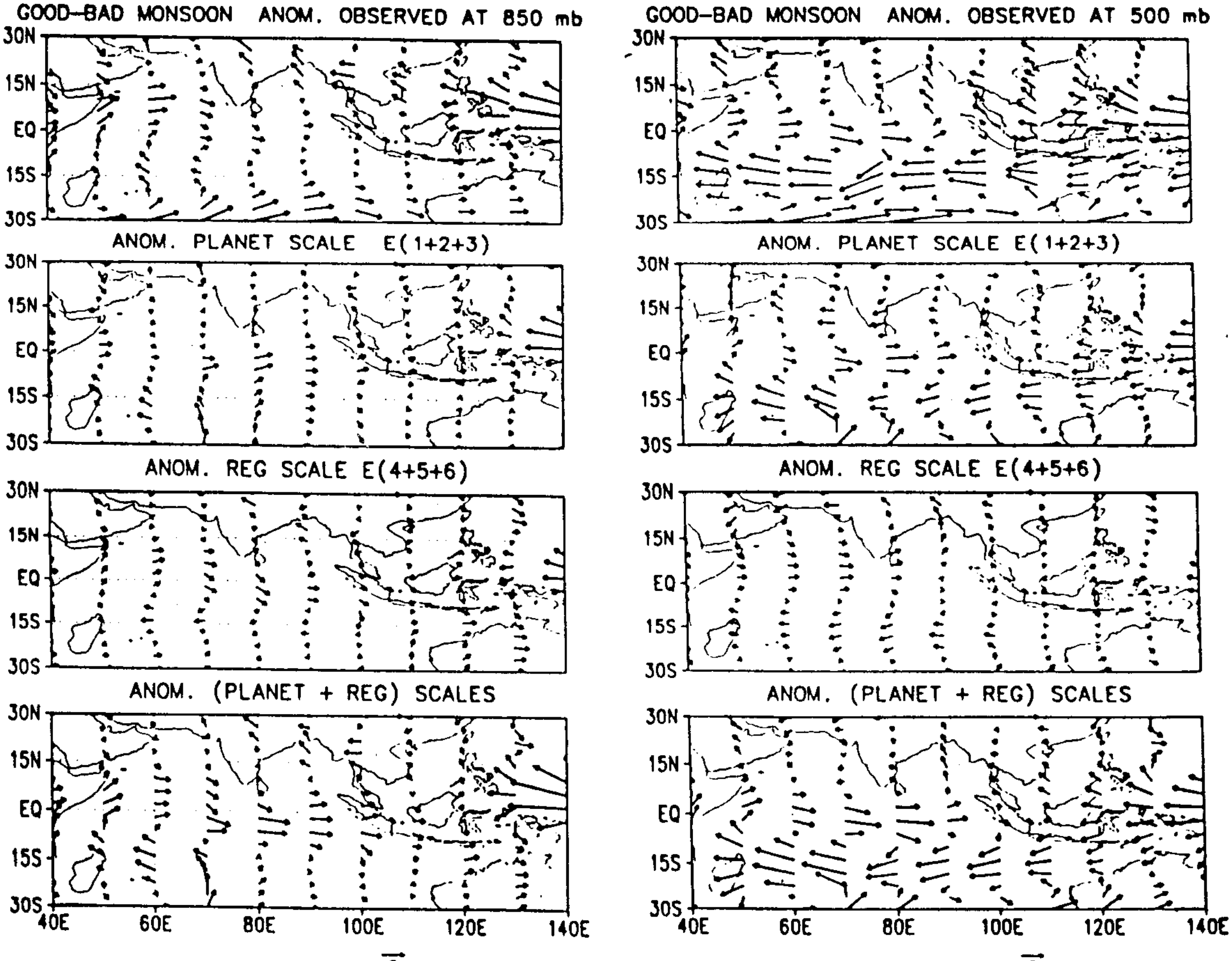

Figure 12: Same as Figure 11 but for winds at

(a) 850 mb (b) 500 mb (c) 300 mb (d) 200 mb

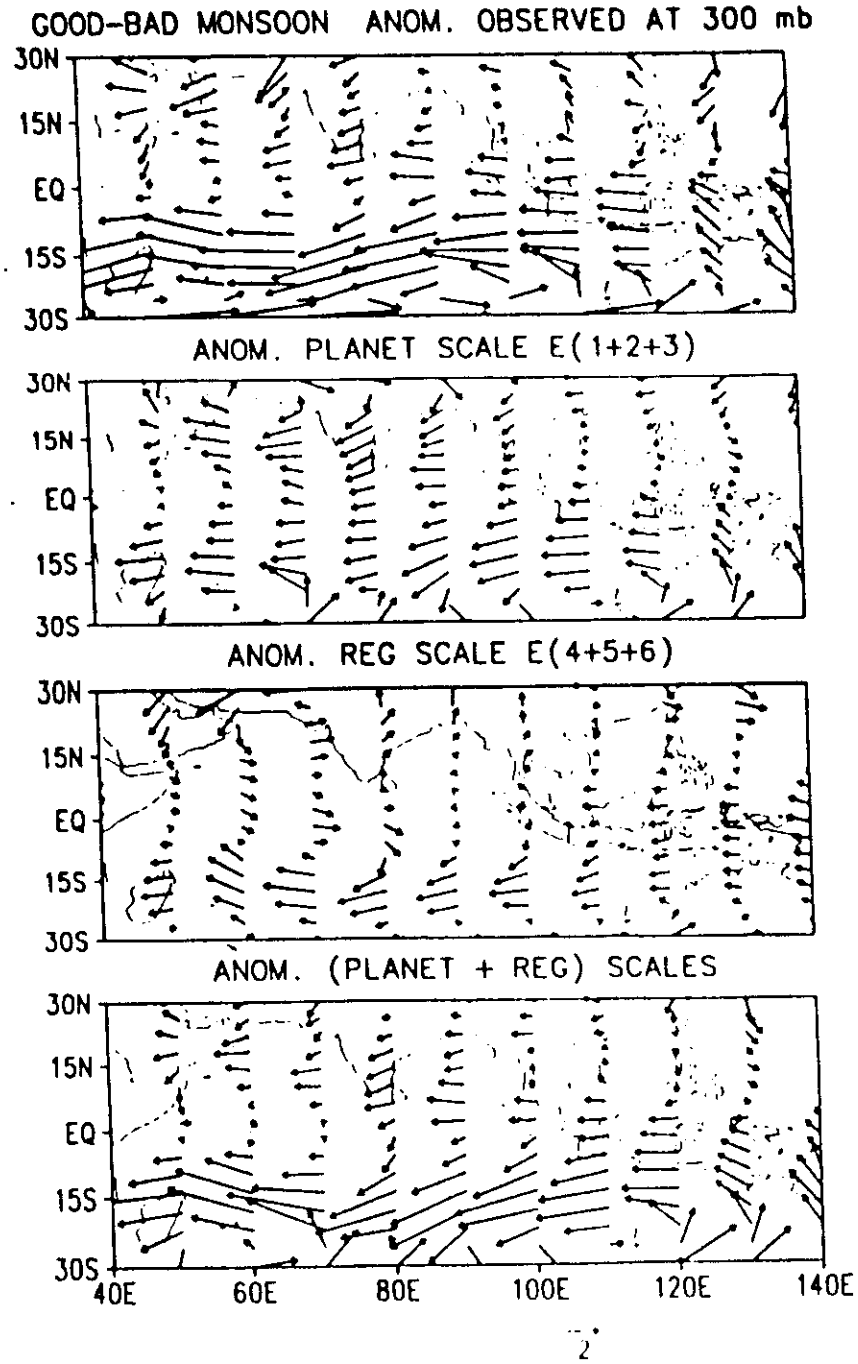
GOOD-BAD MONSOON ANOM. OBSERVED AT 300 mb
ANOM. PLANET SCALE E(1+2+3)
ANOM. REG SCALE E(4+5+6)
ANOM. (PLANET + REG) SCALES
30N
15N
EQ
15S
30S
40E
60E
80E
100E
120E
140E
2

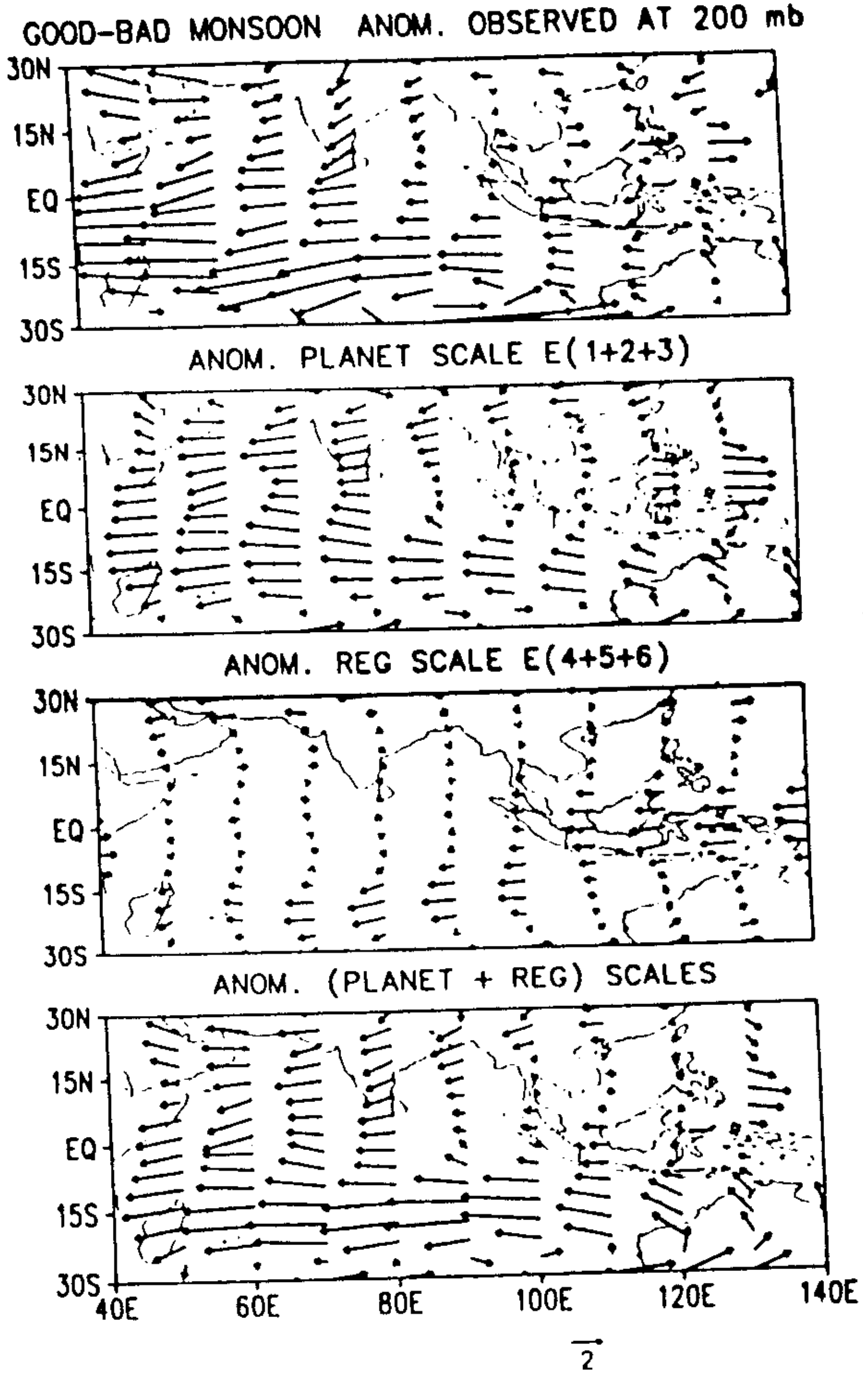
GOOD-BAD MONSOON ANOM. OBSERVED AT 200 mb
ANOM. PLANET SCALE E(1+2+3)
ANOM. REG SCALE E(4+5+6)
ANOM. (PLANET + REG) SCALES
30N
15N
EQ
15S
30S
40E
60E
80E
100E
120E
140E
2

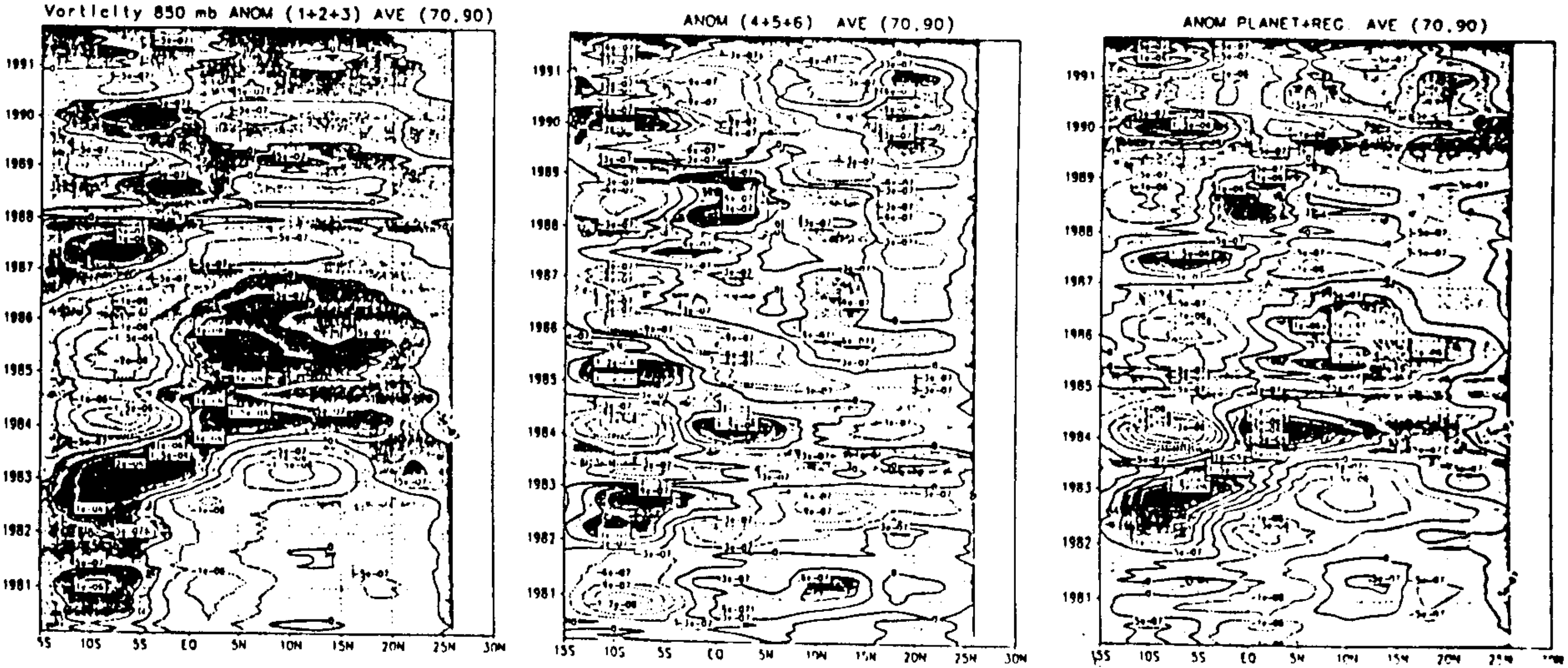

Figure 13: Time-latitude diagram of the relative vorticity at 850 mb averaged over the longitudes ($70°E - 90°E$).

(a) associated with the planetary scale modes

(b) associated with the regional scale modes

(c) sum of the planetary and regional scale modes [13(a) + 13 (b)].

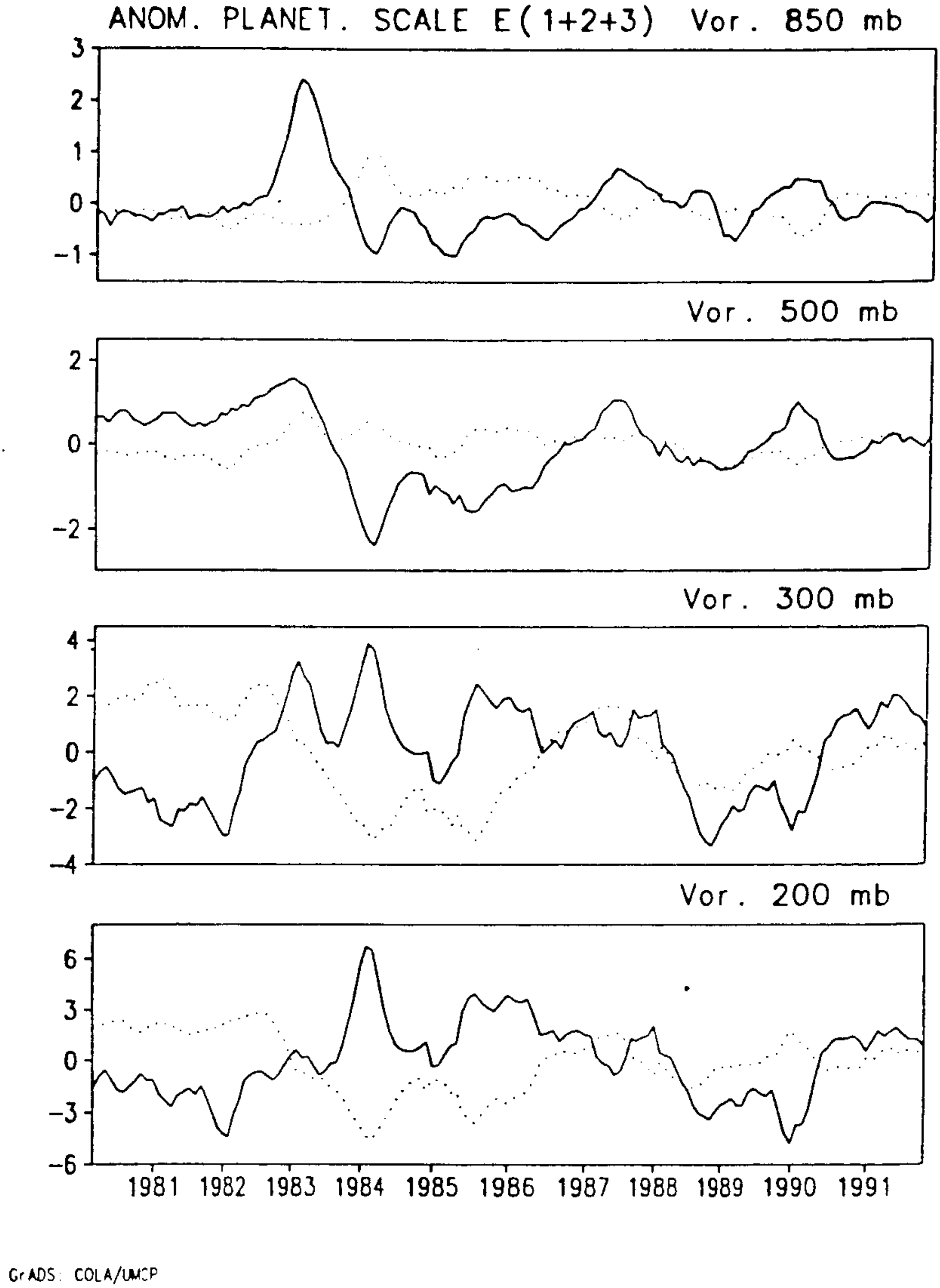

Figure 14: The vertical structure of the relative vorticity. The solid line represents averaged vorticity over the equatorial oceanic area (V_{ocean}), averaged between $10°S-5°N$ and $70°E-90°E$, the dashed line represents the averaged vorticity over the continental area (V_{land}), averaged between $15°N-30°N$ and $70°E-90°E$. All the values are multiplied by 10^6.

(a) associated with the planetary scale modes. For easy comparision.

Level 850 mb: V_{land} is multiplied by a factor of 2,

Level 500 mb: V_{land} is multiplied by a factor of 2,

Level 300 mb: V_{ocean} is multiplied by a factor of 2,

Level 200 mb: V_{ocean} is multiplied by a factor of 2,

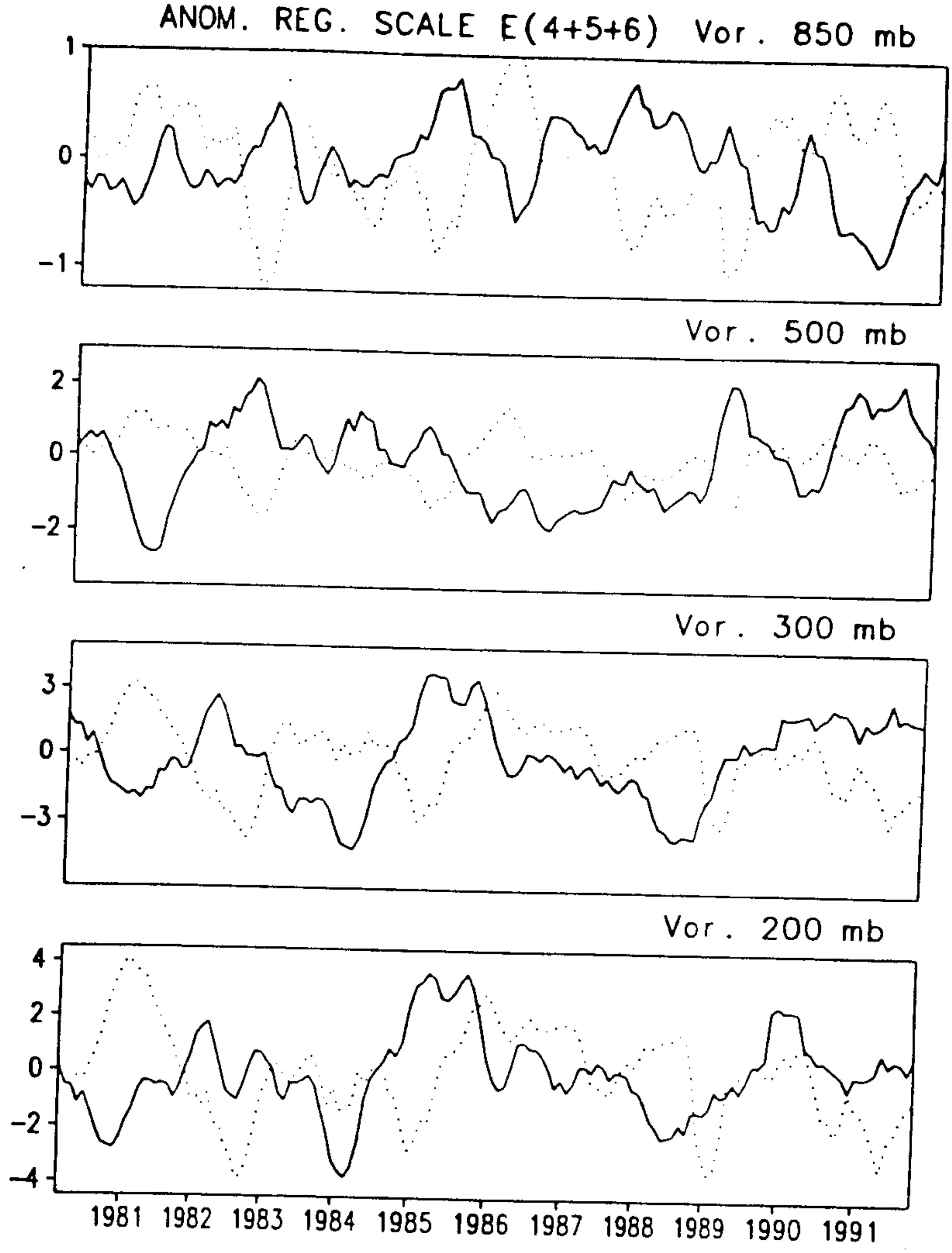

(b) associated with the regional scale modes. For easy comparision,
Level 300 mb: V_{ocean} is multiplied by a factor of 2,
Level 200 mb: V_{ocean} is multiplied by a factor of 2,

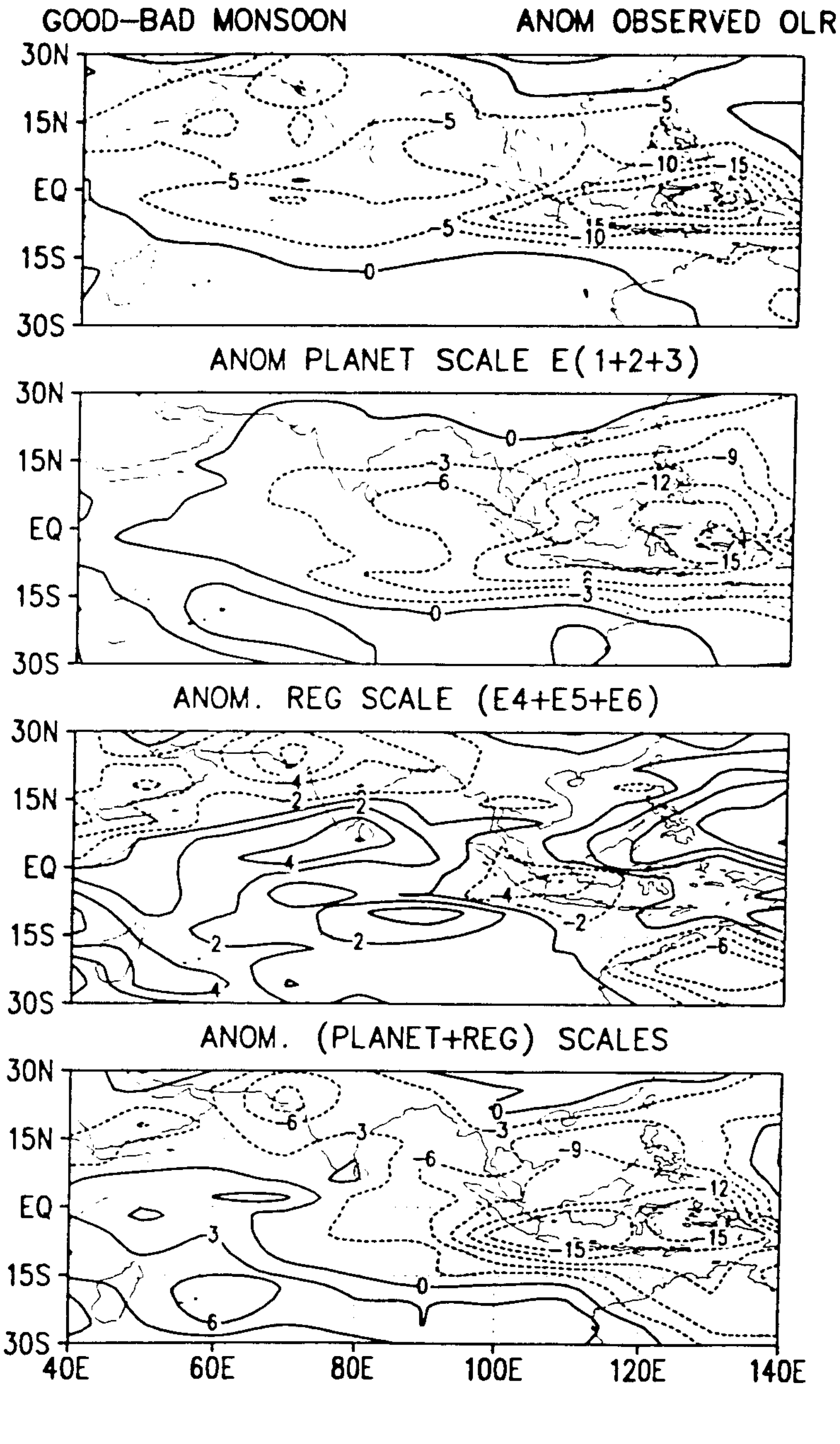

Figure 15: Same as Figure 11 but for OLR.